Radar Measurement of Precipitation from Space:
TRMM/PR and GPM/DPR rain retrieval algorithms

Toshio Iguchi

National Institute of Information and Communications Technology

Riken, Kobe, 26 June 2017

Remote sensing of rain by radar

RADAR: RAdio Detection And Ranging

- Radar emits a known pulse of radio waves and measures its echoes from objects or targets.
- The time for the pulse to travel to the target gives the distance to the target.
- The direction of the radio waves gives the direction of the target.
- The echo power depends on the size and number of the targets.

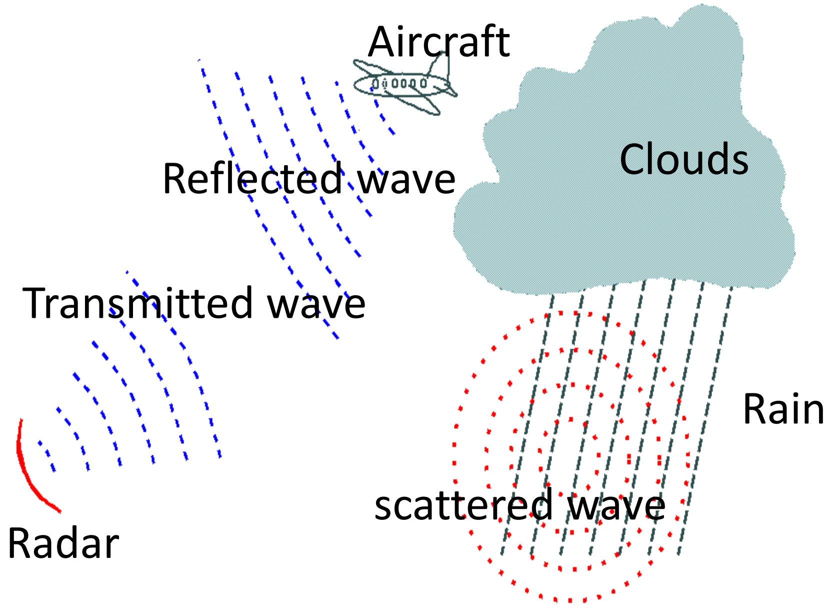

TRMM Sensors

Precipitation radar (PR):

- 13.8 GHz
- 4.3 km footprint
- 0.25 km vertical res.
- 215 km swath

Microwave radiometer (TMI):

- 10.7, 19.3, 21.3, 37.0 85.5 GHz (dual polarized except for 21.3 V-only)
- 10 x 7 km FOV at 37 GHz
- 760 km swath

Visible/infrared radiometer (VIRS):

- 0.63, 1.61, 3.75, 10.8, and 12 μm at 2.2 km resolution

Additional EOS instruments:

CERES (Cloud & Earth Radiant Energy System) 720 km swath

LIS (Lightning Imaging Sensor)

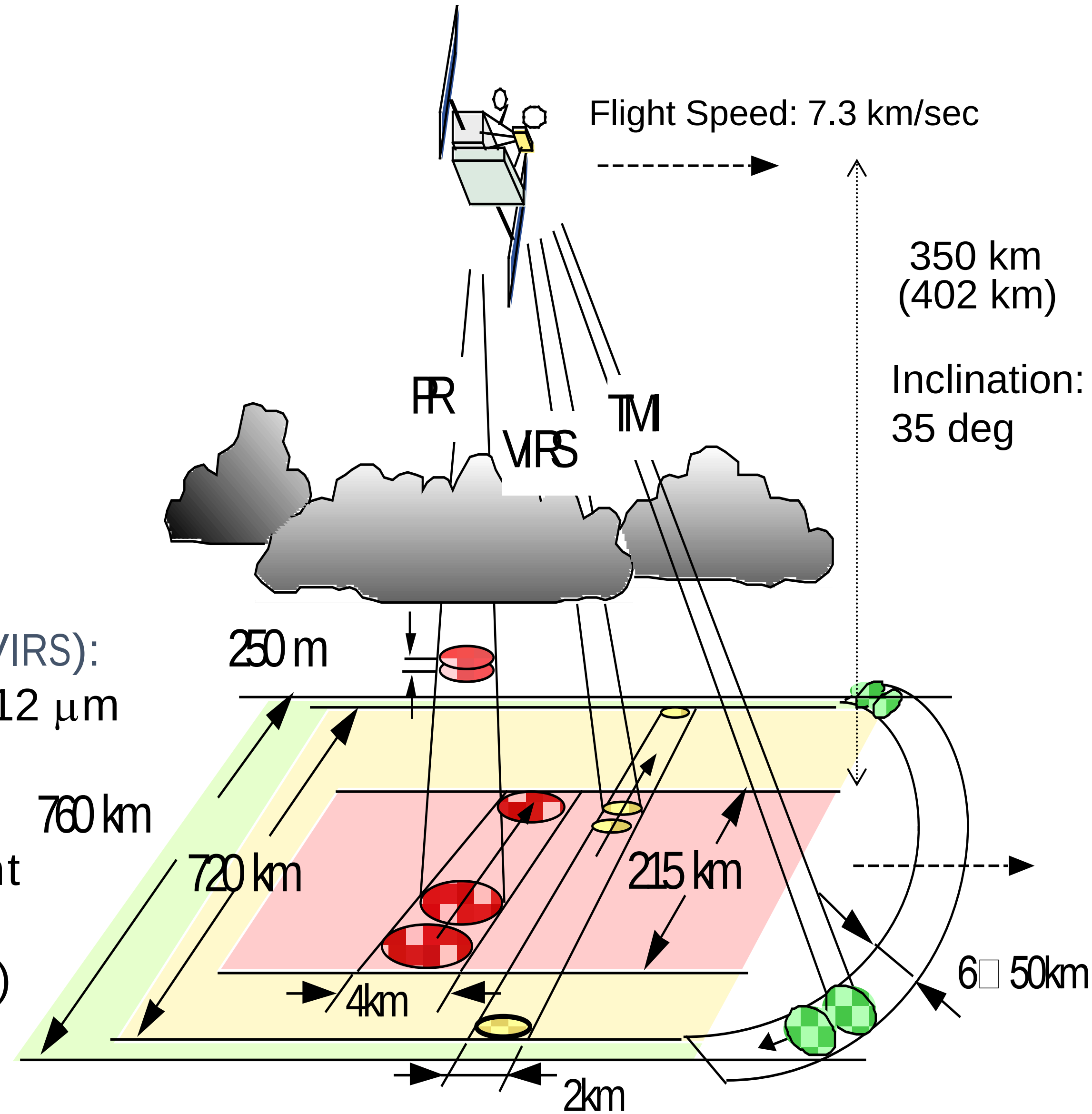

TRMM Precipitation Radar

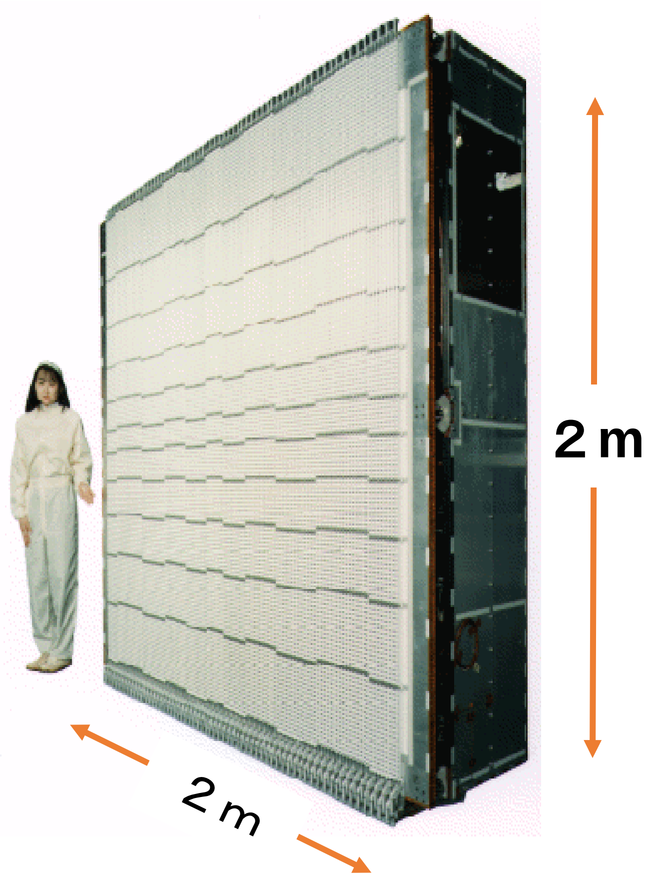

Radar type	Pulse radar
Antenna type	128-elem. WG slot array
Beam scanning	Active phased array
Frequency	13.796, 13.802 GHz
Polarization	Horizontal
TX/RX pulse width	1.57 / 1.67μsec
RX band width	0.6 MHz
Pulse rep. freq.	2776 Hz
Data rate	93.5 kbps
Mass	460 kg
Designed Life time	3 years
Sensitivity	< 0.5mm/h
Horizontal resolution	4.3 km (nadir)
Range resolution	250 m
# of indpdt samples	64 (fading noise < 0.7 dB)
Swath width	215km
Observable range	Surface to 15km

A squall line observed with TRMM PR and VIRS

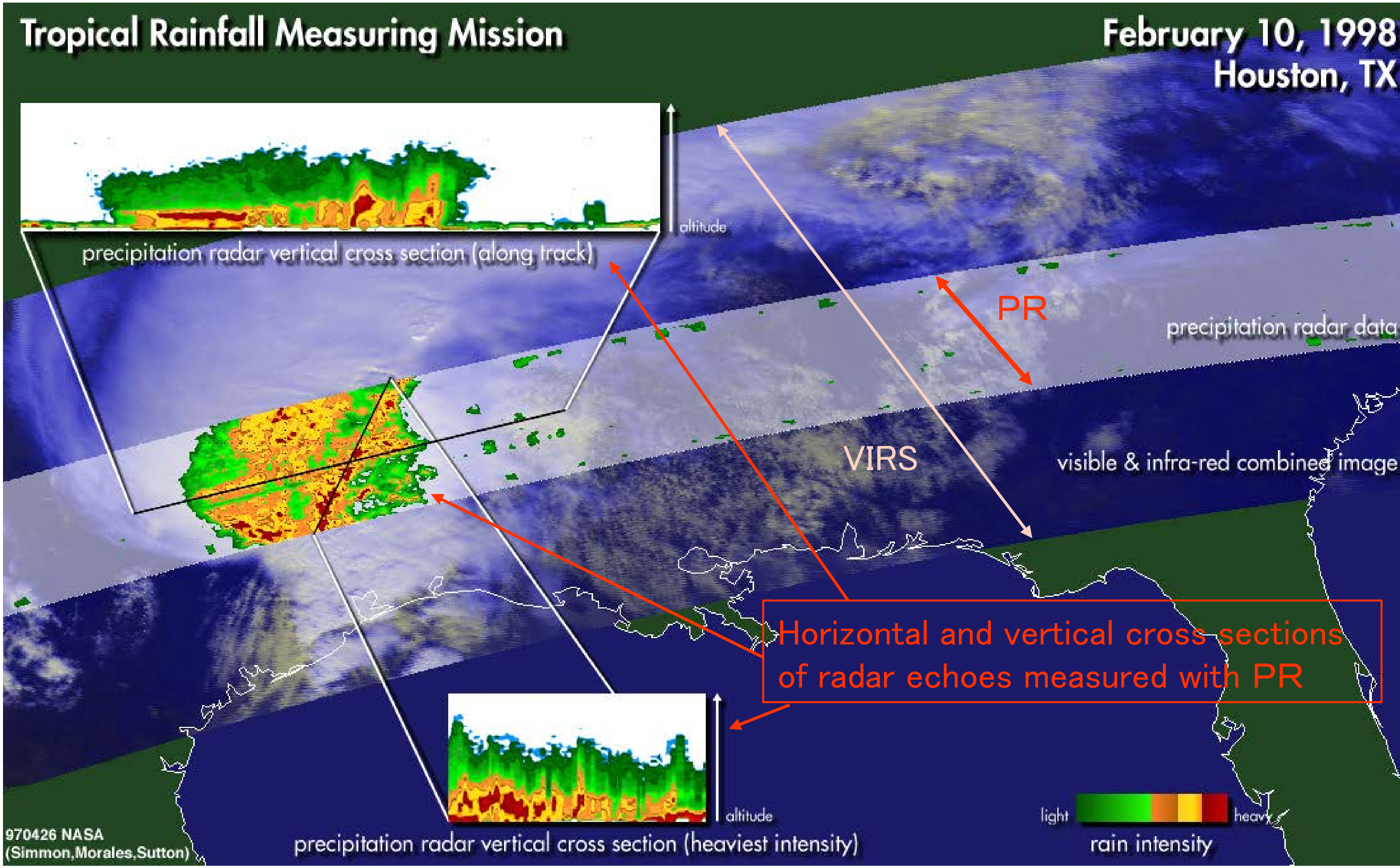

3-D Observation of a Typhoon by the PR

TRMM PR 2A25 Rain

Aug. 2, 2000, 20:49-20:53 (Japanese local time)

Rain intensity at H=2 km

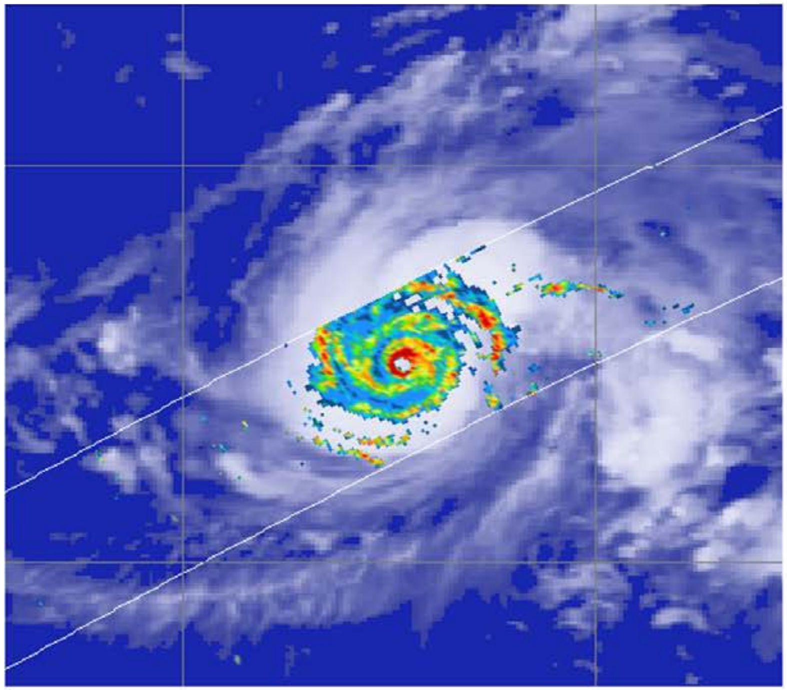

Vertical cross section through the eye and 3D structure

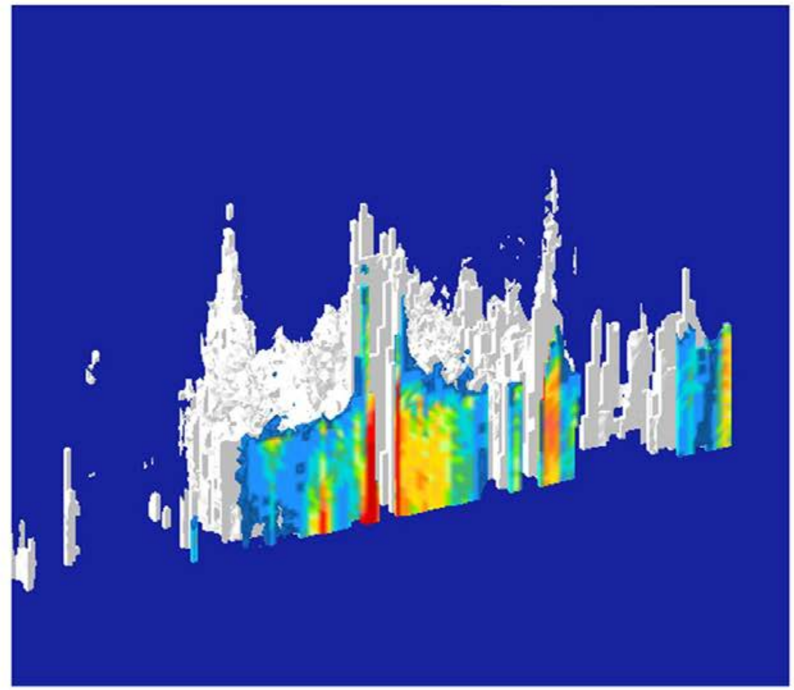

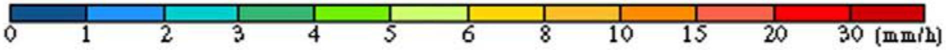

PR realized observation of 3D structure of rain over ocean where few observations had been available.

Monthly Rain Distributions estimated from the TRMM PR data in 1998 (El Nino year) and 1999

El Nino year (January 1998, Height=2km)

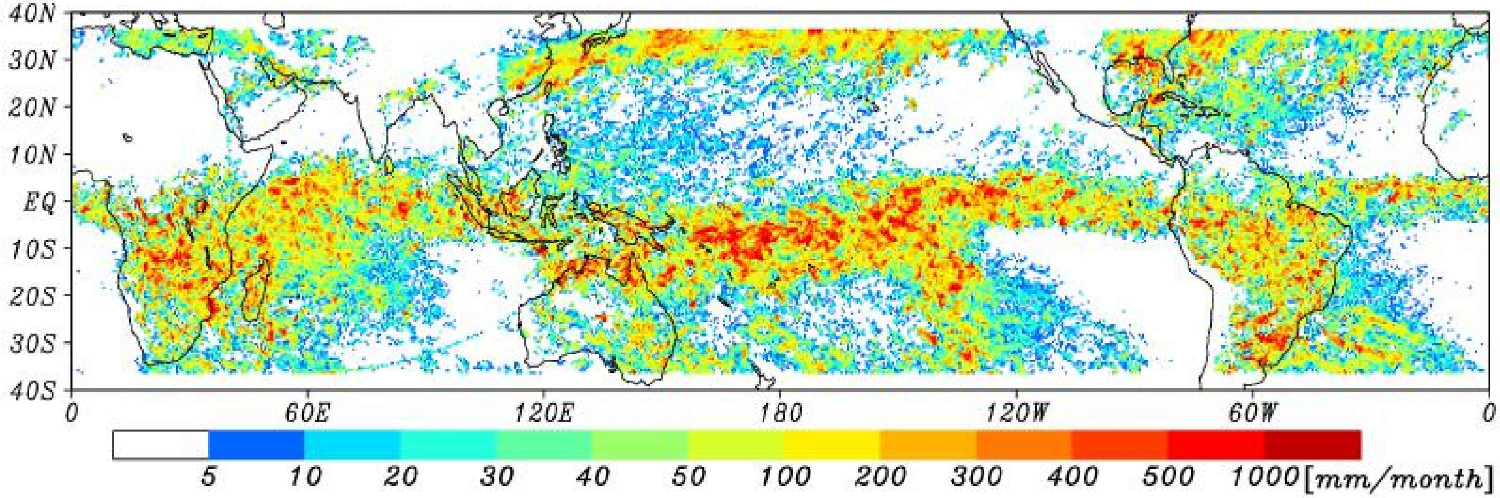

Ordinary year (January 1999, Height=2km)

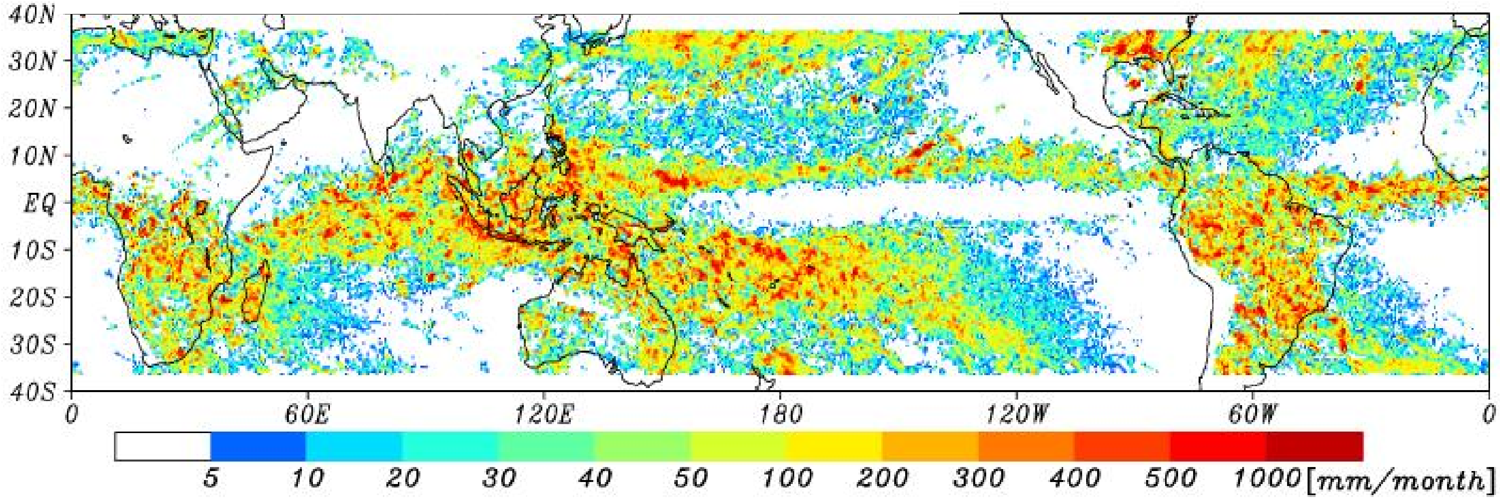

Strom Top Height Distribution measured with the TRMM Precipitation Radar

Boreal summer (July 1998, Height=2km)

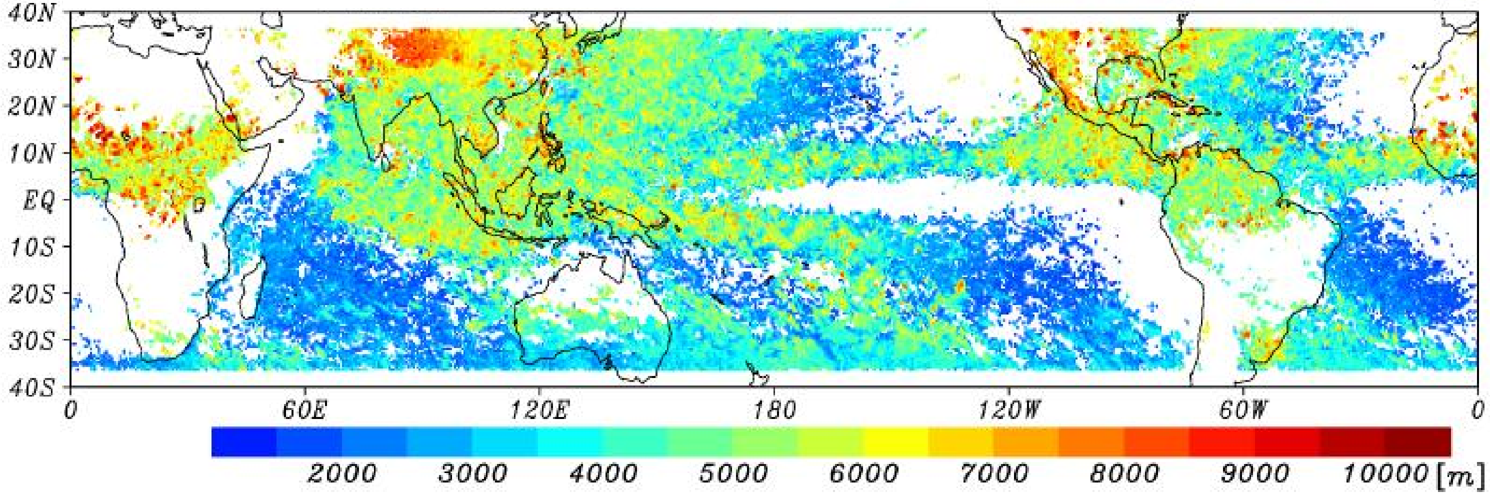

Austral summer (January 1999, Height=2km)

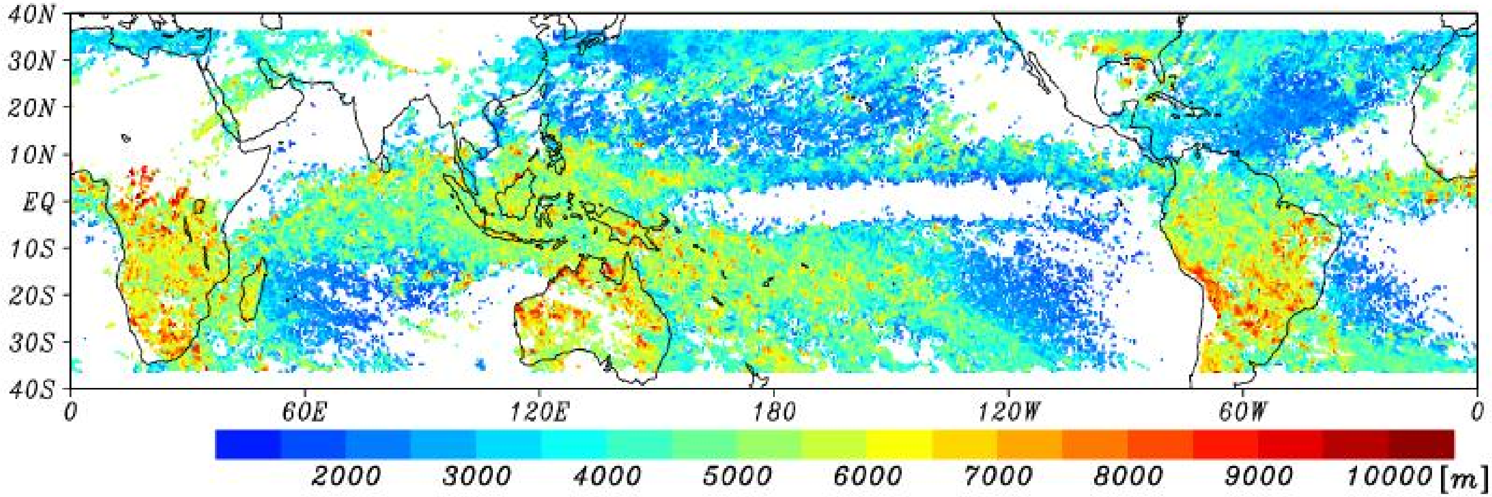

TRMM PR climatology

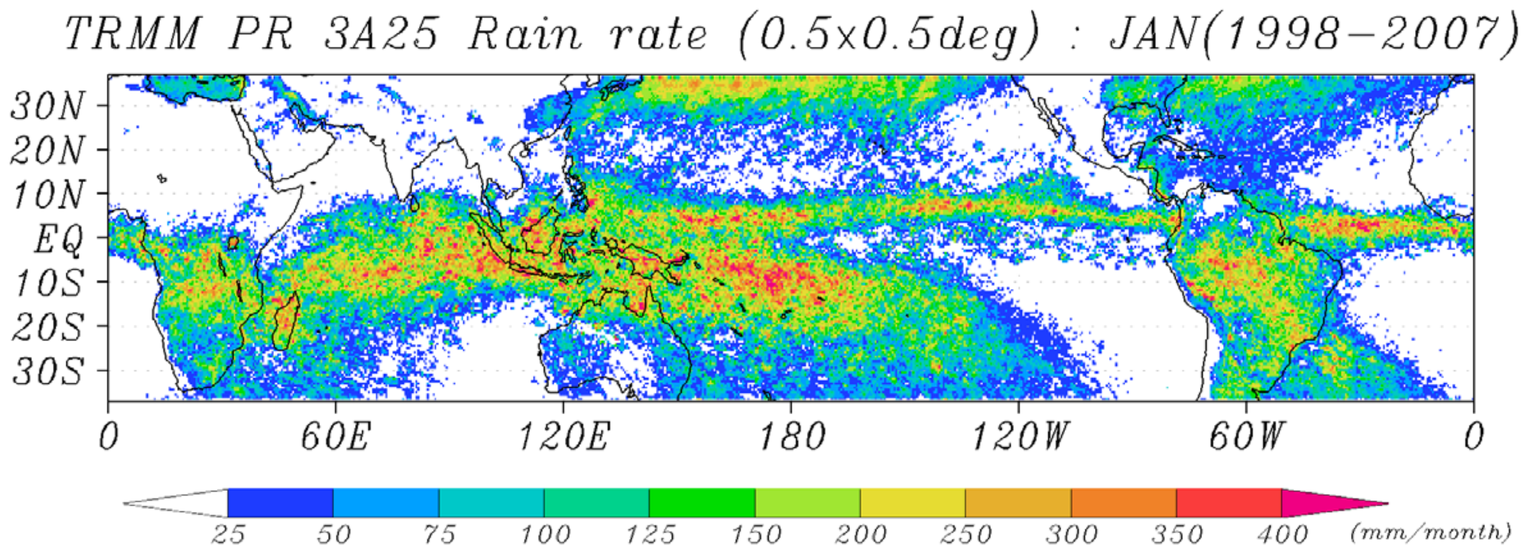

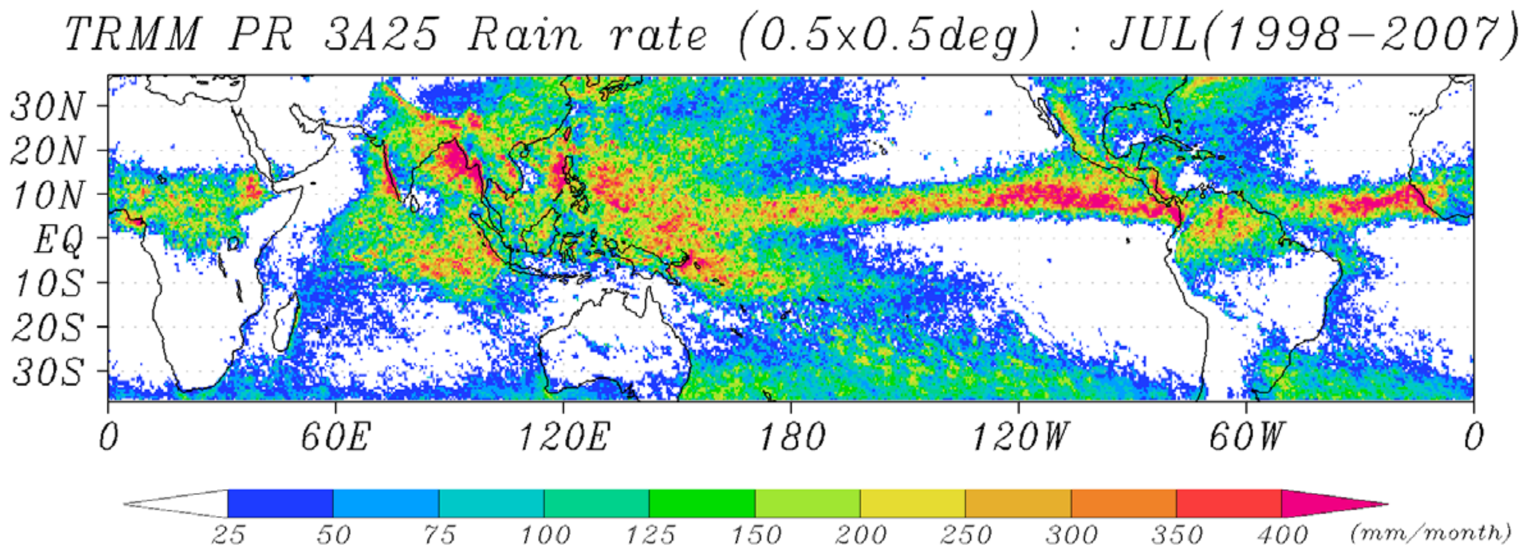

Improvement in weather forecasts

4D-VAR assimilation in the JMA meso-scale model

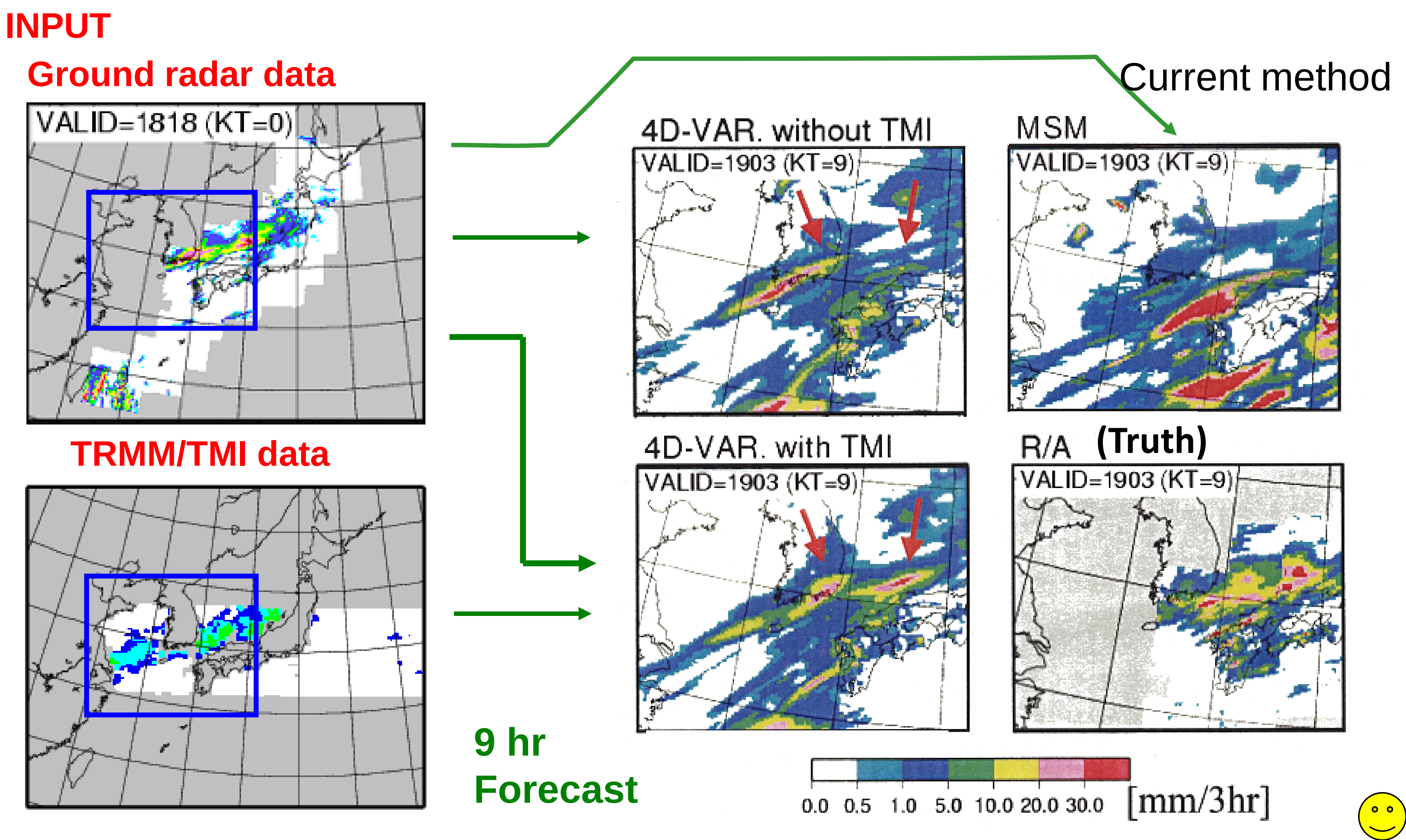

Peculiarities of satellite-borne radar

Differences from ground-based radar

- Hardware constraints
  - size (<2 m), mass, power consumption
    - use of short waves -> attenuation (rain, snow, water vapor, cloud liquid water, and oxygen molecules)
    - sensitivity
  - reliability
- Observation geometry
  - distance (>300 km), angle
    - sensitivity, resolution
  - surface behind rain
    - surface clutter
  - moving platform (unless from a geostationary satellite)
    - difficulty in Doppler measurement
- Other factors
  - Sparse sampling in time at a given location
  - Various rain systems with different characteristics
  - Excellent stability (<0.1dB change since launch)
    - can be used as a calibrator of ground-based radars

Footprint size and wavelength

- Use of relatively high frequency (short wave) to realize a good horizontal resolution.
  - antenna beam width ~ $c_1\lambda/D$ (wavelength/diameter)
    - λ: wavelength of the electromagnetic wave
    - D: antenna diameter
    - c_1: a constant that depends on the antenna illumination (~1.2)
  - footprint size ~ $c_1 r\lambda/D$ (r: range to surface)
  - D < 2~3 m unless the antenna is developed on orbit
  - r > ~300 km.
  - -> use a small λ to make the footprint size ($c_1 r\lambda/D$) small.
  - to realize a 5 km footprint with a 2 m antenna from a 400km orbit, λ ~ 5*2/(1.2*400) m = 2.08 cm (= 14.4GHz)

Radar Equation

$$P_r(r) = P_t \frac{G_t G_r \lambda^2 \theta_1 \theta_2 c\tau}{2^{10}\pi^2 \ln(2) r^2} \eta(r) \exp(-2 \int_0^r k(s)\, ds)$$

$$\eta = \frac{1}{V} \sum_V \sigma_b = \int \sigma_b(D) N(D) dD$$

$$k = \frac{1}{V} \sum_V \sigma_t = \int \sigma_t(D) N(D)\, dD$$

$$Z_e = \frac{\lambda^4}{\pi^5 |K_w|^2} \eta, \qquad K = \frac{\epsilon_r - 1}{\epsilon_r + 2} = \frac{n^2 - 1}{n^2 + 2}$$

$$R = \frac{\pi}{6} \int D^3 v(D) N(D)\, dD \overset{\propto}{\approx} \int D^{3.67} N(D)\, dD$$

If $\lambda \gg \pi D$ (Rayleigh scattering),

$$\eta \propto \int D^6 N(D)\, dD = Z, \qquad k \propto \mathrm{Im}(-K) \int D^3 N(D)\, dD$$

Drop Size Distribution (DSD)

- Both *k-Ze* and *R-Ze* relations depend on DSD.
- Hitschfeld-Bordan's solution assumes a *k-Ze* relation.
- When the SRT is not applicable, the initial DSD determines the attenuation correction and the *Ze*-to-*R* conversion.
- When the SRT is applicable, α can be adjusted to match the H-B estimate of PIA to the SRT PIA. This in effect corresponds to adjusting the initial DSD.

Hitschfeld-Bordan solution

$$Z_m(r) = Z_e(r) \exp\left(-0.2 \ln 10 \int_0^r k(s)\, ds\right)$$

If $k = \alpha Z_e^{\beta}$, then

$$Z_e(r) = \frac{Z_m(r)}{\left(C_1 - 0.2 \ln(10) \beta \int_0^r \alpha(s) Z_m^{\beta}(s)\, ds\right)^{1/\beta}}$$

DSD variation in Indian rain

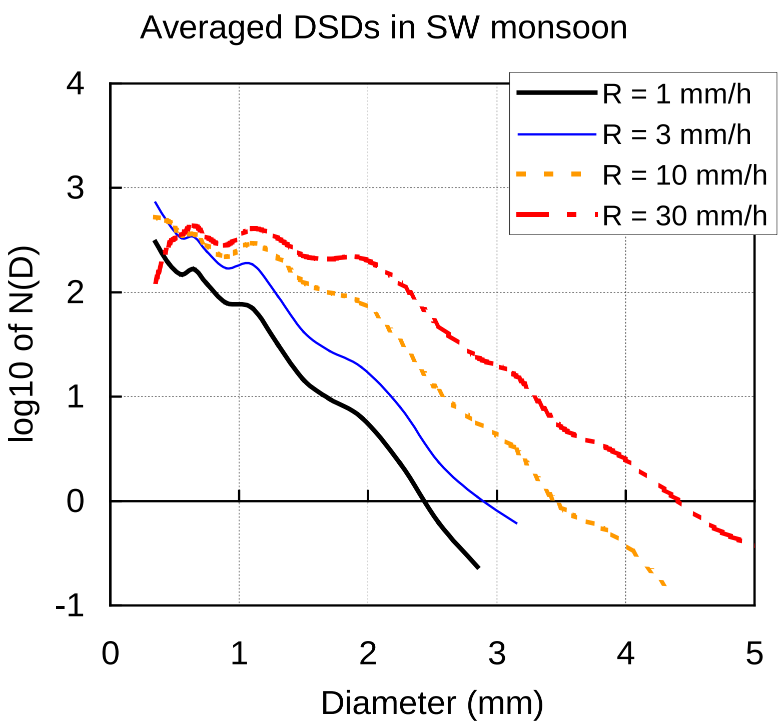

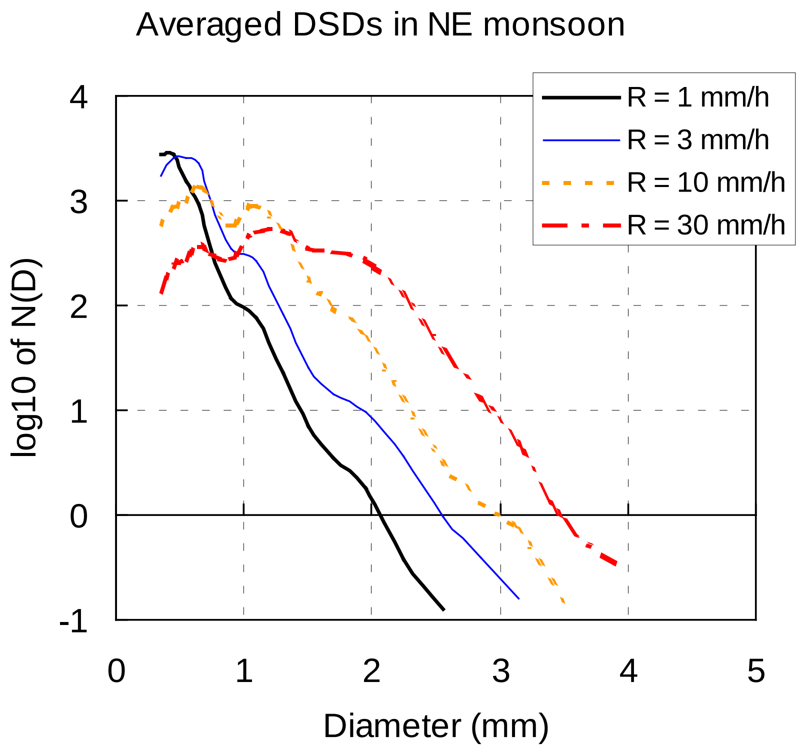

Averaged Dropsize Distribution during South-West (SW) and North-East (NE) monsoon seasons in Gadanki, south India in 1997 and 1999. SW and NE seasons are between May and October, and between November and December, respectively. DSDs within +/- 1 dB centered at the rain rate specified are averaged.

T. Kozu, K. K. Reddy and A.R. Jain
Oct. 20, 2000

Z-R relations
in SW and NE Indian monsoon seasons

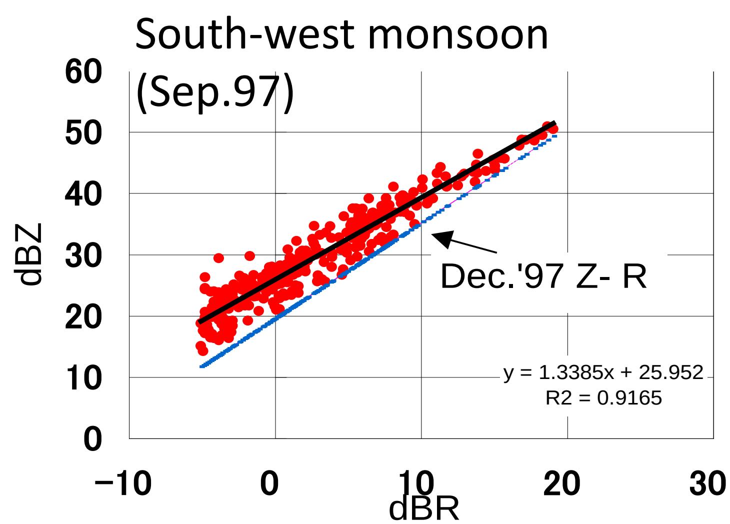

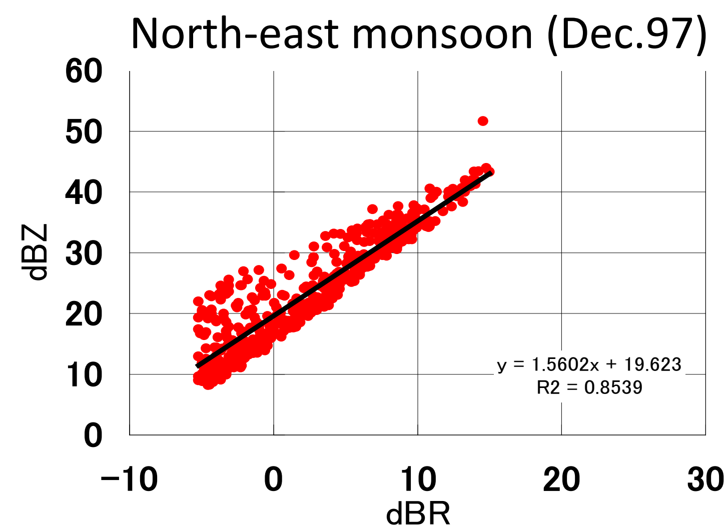

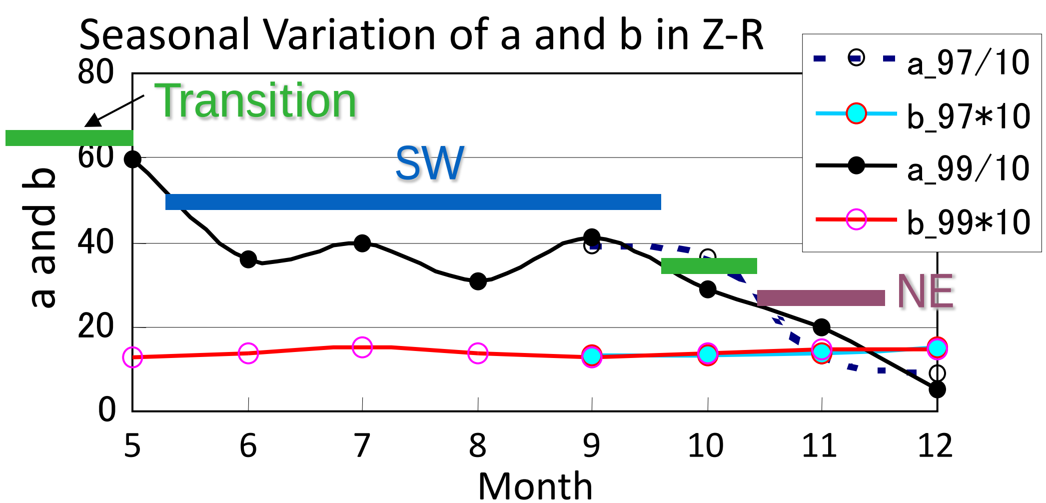

SW $Z = 405R^{1.29}$

NE $Z = 144R^{1.38}$

Strat/Conv separation:
Not significant

Surface clutter

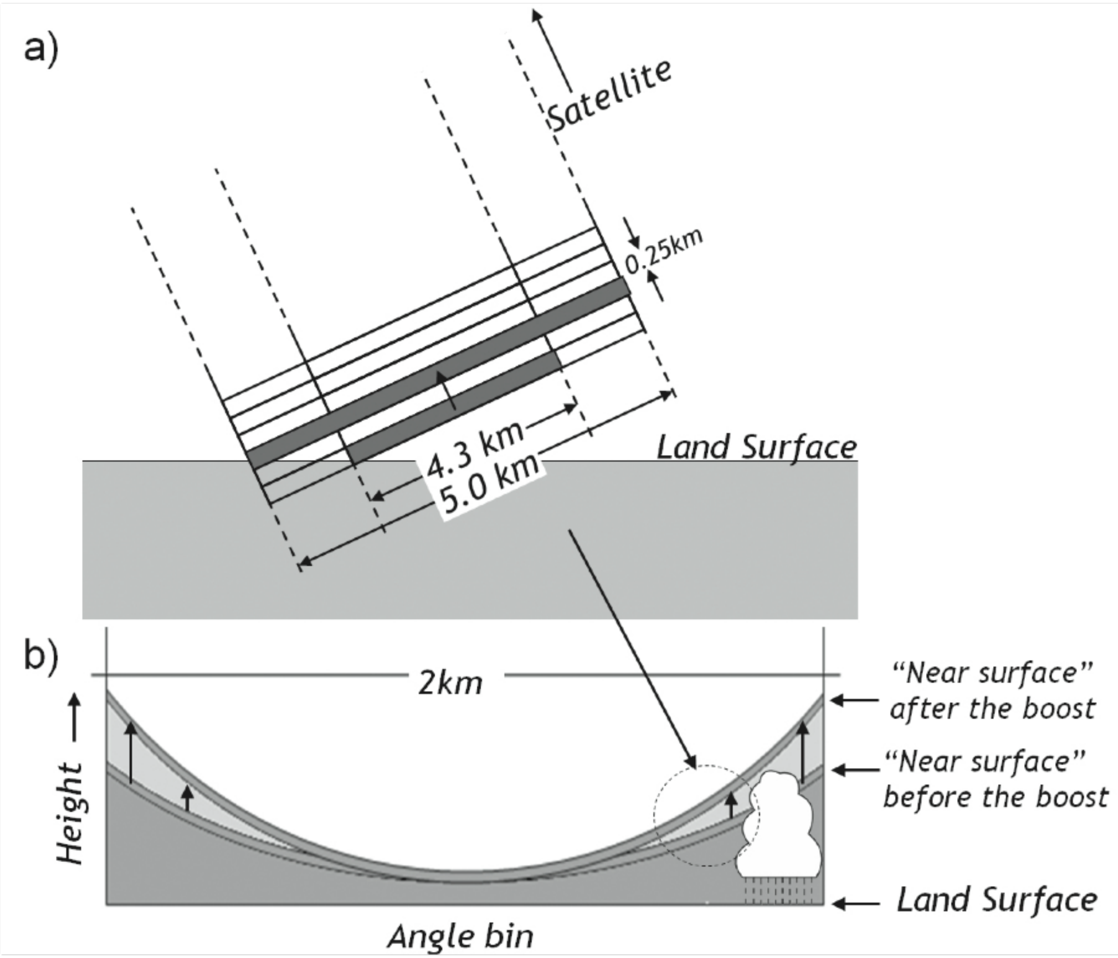

Shmizu et al. (2009)

Other issues due to the nature of the measurements

- main lobe and side lobe clutter obscuring the near surface echo, can contaminate meteorological echo
- Uncertain σ_0 in complex terrain
- *A priori* DSD assumed as a function of height. Appropriate?
- Single frequency measurements + unreliable PIA = limited independent DSD information

Surface Reference Technique

Decrease of the apparent surface echo ($\Delta\sigma^0$) under rain is interpreted as the path-integrated attenuation (PIA) due to rain.

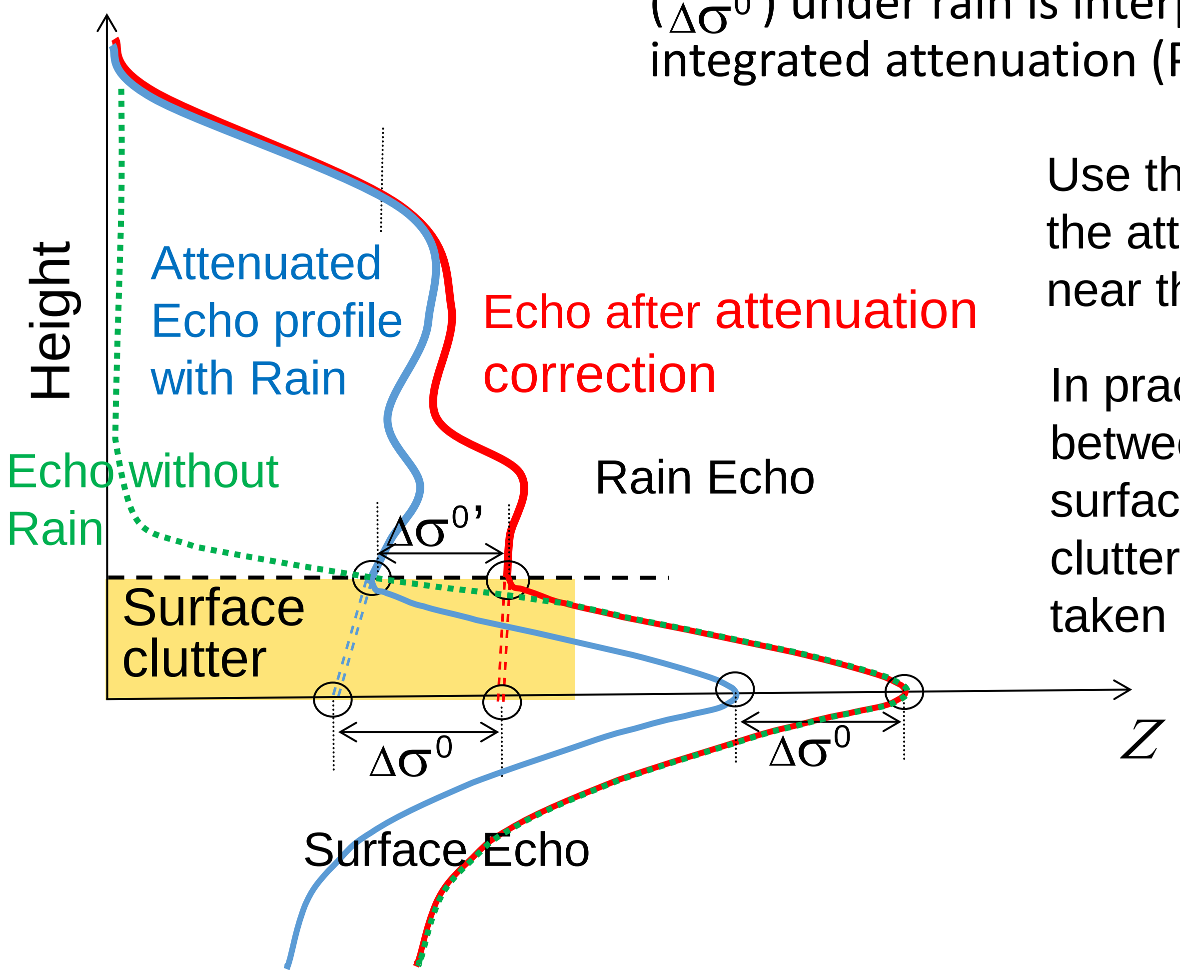

Use this PIA to correct for the attenuation of rain echo near the surface.

In practice, the difference between the PIA to the surface and the PIA to the clutter-free bottom must be taken into account.

Rain and Surface Echoes

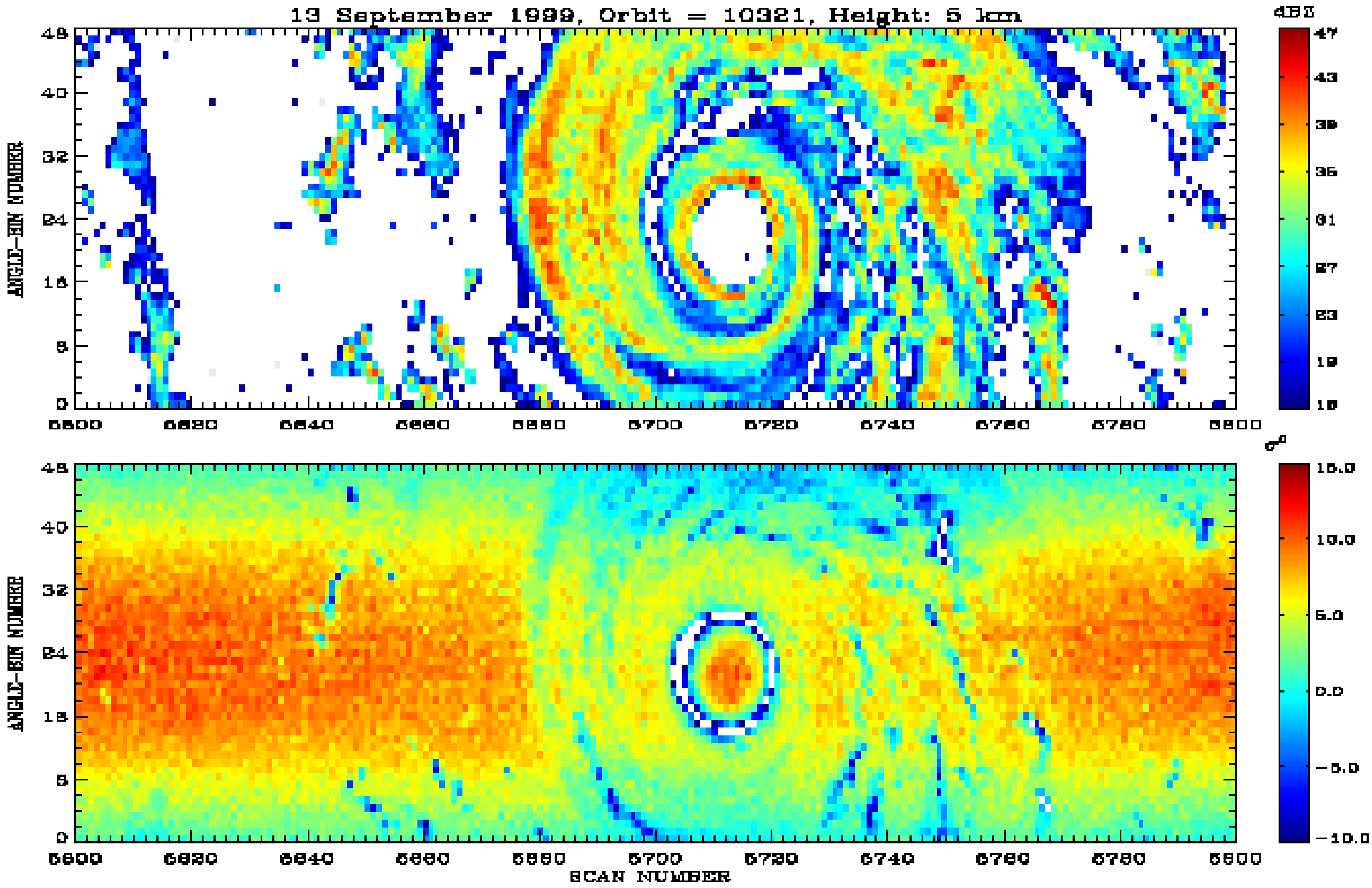

Vertical Cross Section of Radar Echo and Decrease of Apparent Surface Cross Section

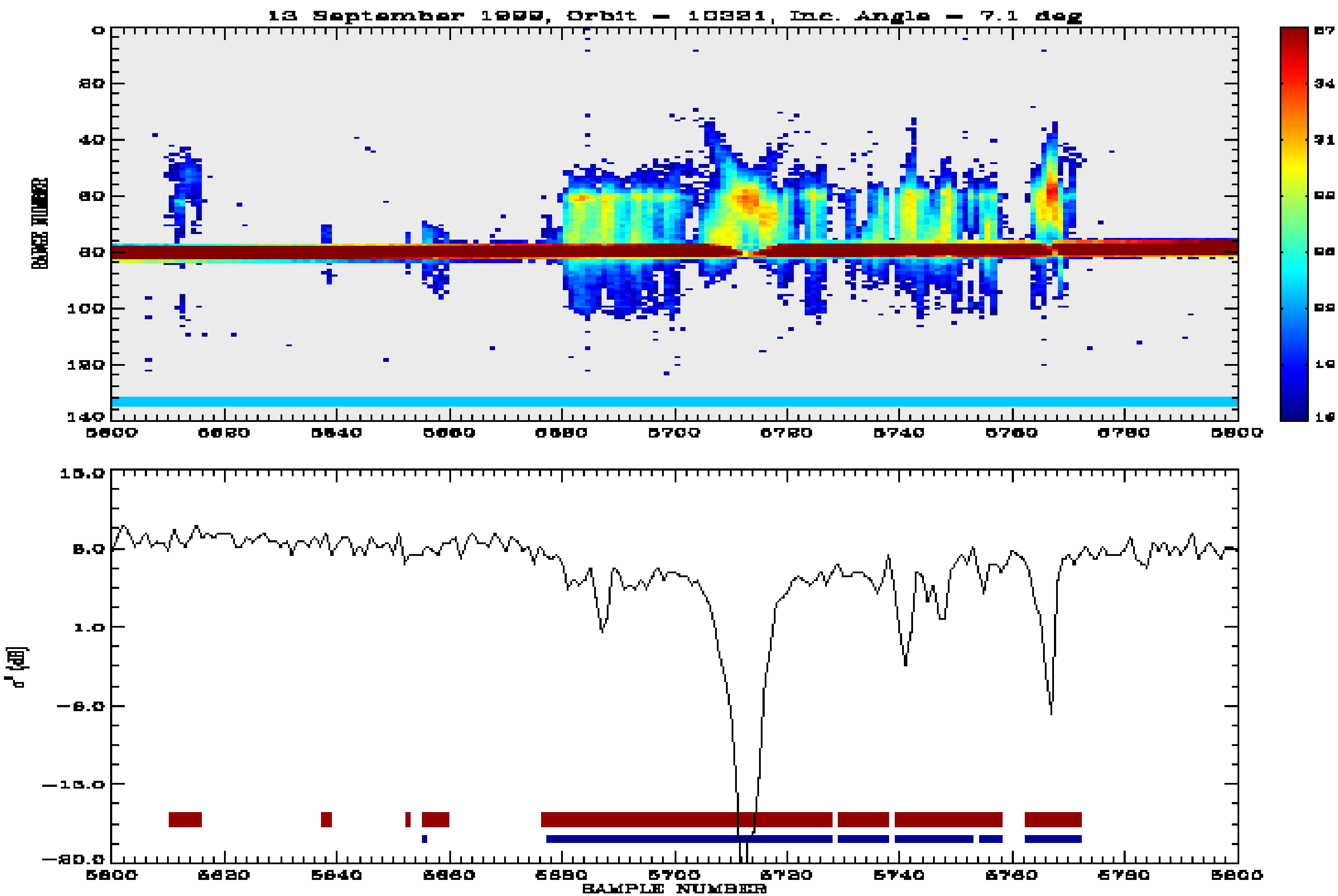

(R. Meneghini)

TRMM/PR Standard Algorithm

$$Z_m(r)=Z_e(r)\exp\left[-0.2\ln(10)\int_0^r k(s)ds\right]$$

$$k(r)=\alpha_0(r)Z_e(r)^{\beta_0}$$

DSD assumed

$$Z_e(r_s)=Z_m(r_s)/(1-\zeta)^{1/\beta_0}$$

$$\zeta=0.2\beta_0\ln(10)\int_0^{r_s}\alpha_0(s)Z_m(s)^{\beta_0}ds$$

$$\mathrm{PIA}_{\mathrm{HB}}=-\frac{10}{\beta_0}\log_{10}(1-\zeta)$$

Hitschfeld-Bordan (HB)

$$\mathrm{PIA}_{\mathrm{fin}}=-\frac{10}{\beta_0}\log_{10}(1-\varepsilon\zeta)$$

Bayesian

$$\mathrm{PIA}_{\mathrm{SRT}}=\sigma^0_{\mathrm{SRT}}-\sigma^0_{\mathrm{m}}$$

Surface Reference Technique (SRT)

σ^0_{SRT} is an estimate of σ^0_e

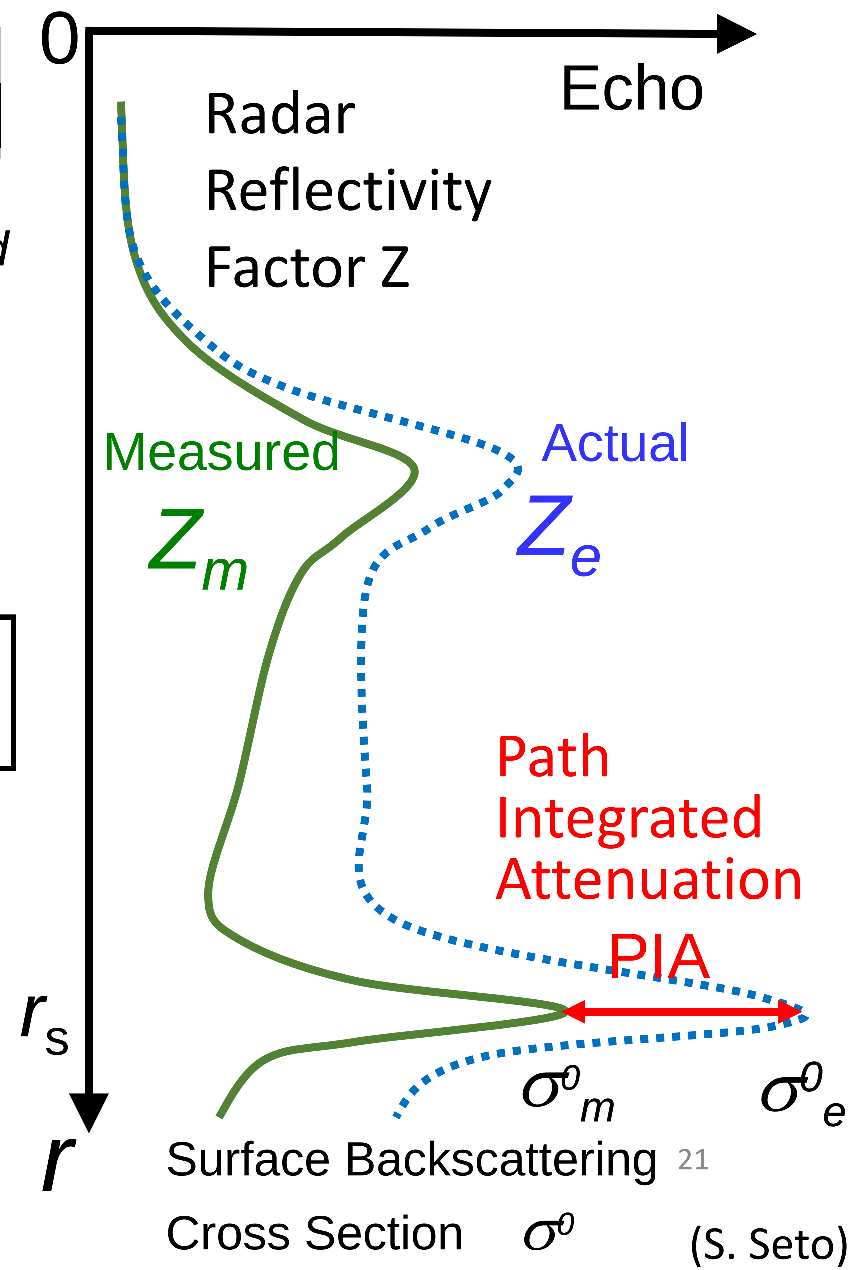

(S. Seto)

k profiles for Z_e=40 dBZ

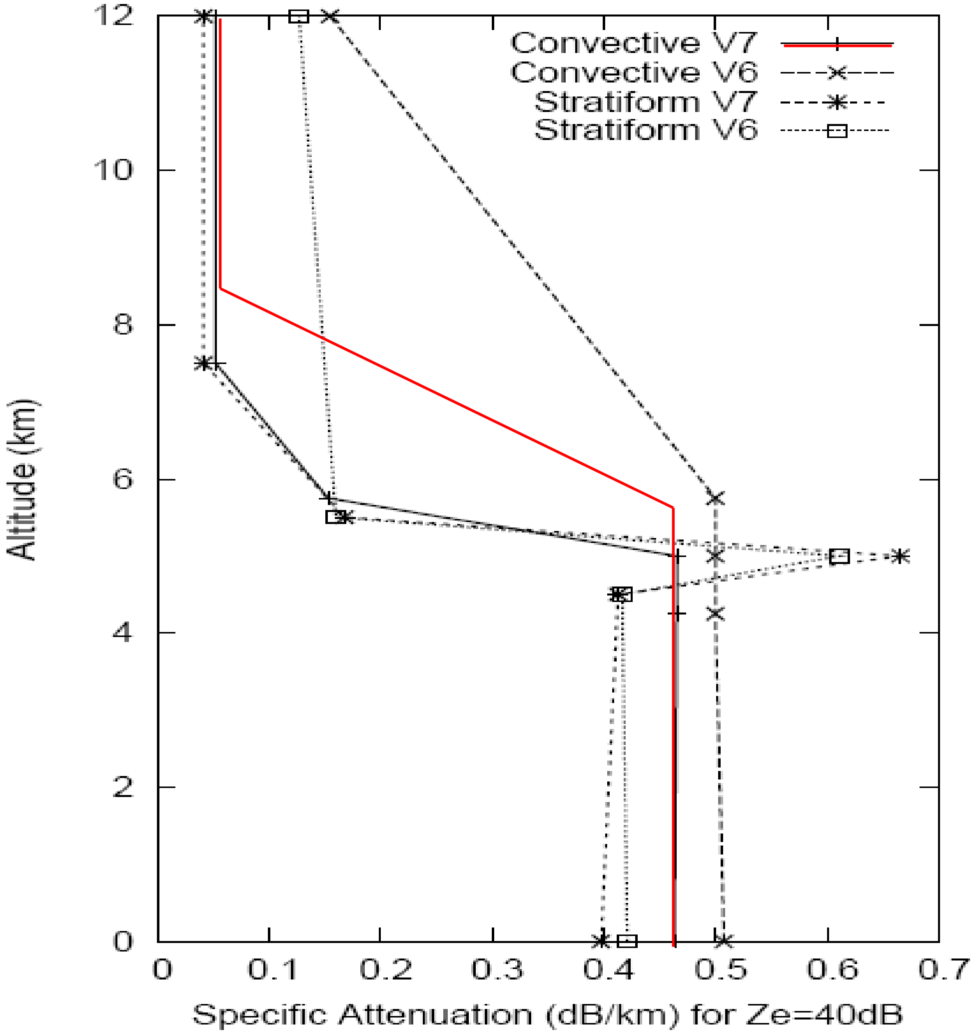

0 degree C height is assumed at 5 km
The lapse rate is assumed to be -6 degrees/km.

The assumed profile has been changed to the red line in V7 (ITE232).
(100% ice above the -20 degree level.)
It was the solid line before the change
(100% ice above the -15 degree level.)

PR Algorithm Flow and adjustable parameters

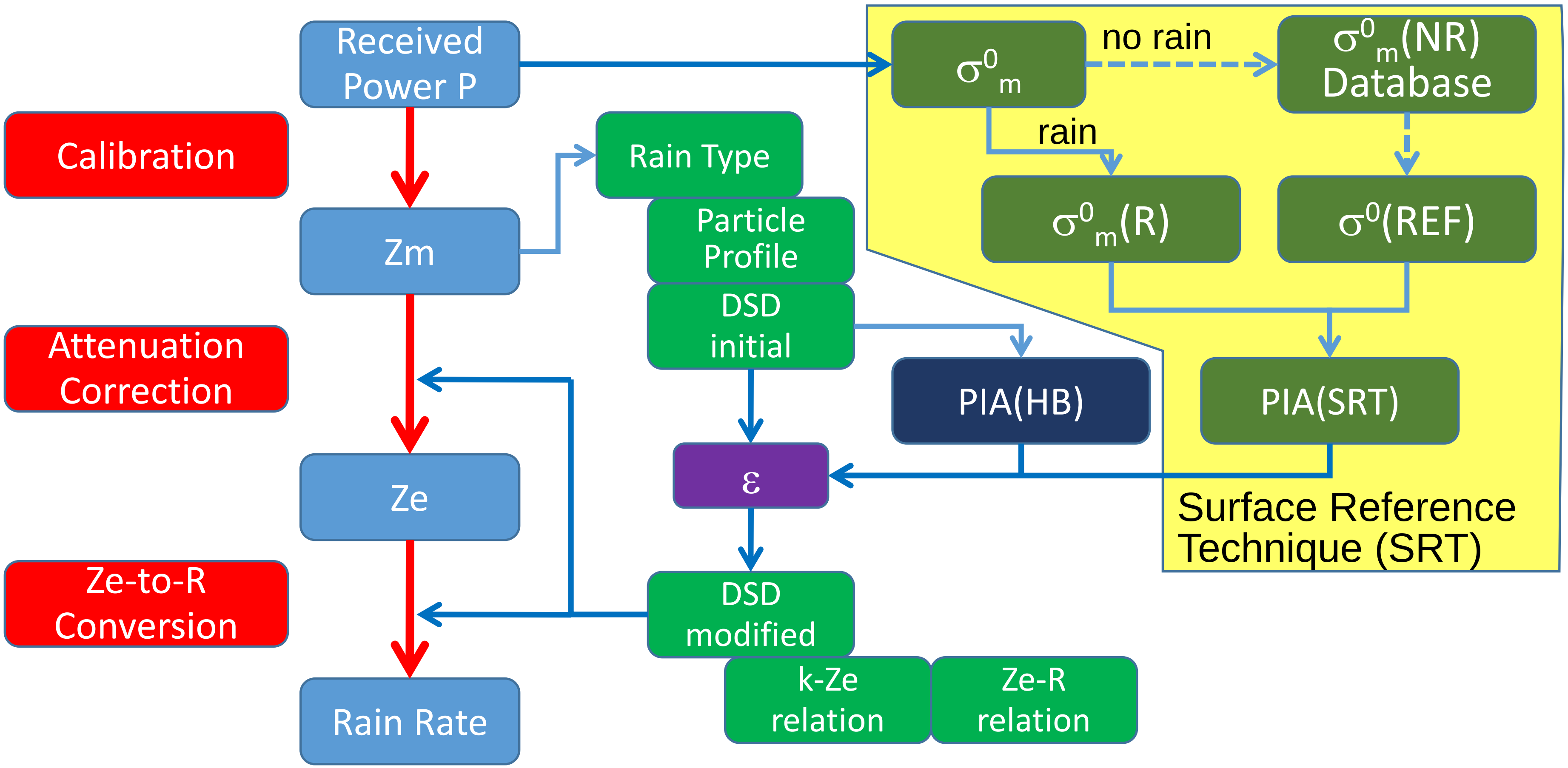

- Calibration
- Particle model
  - DSD parameters
  - particle profile
    - BB model
    - snow model

- Measurement errors
- PIA errors
- Rain profile in surface clutter
- Inhomogeneity

Effect of non-uniform rain distribution

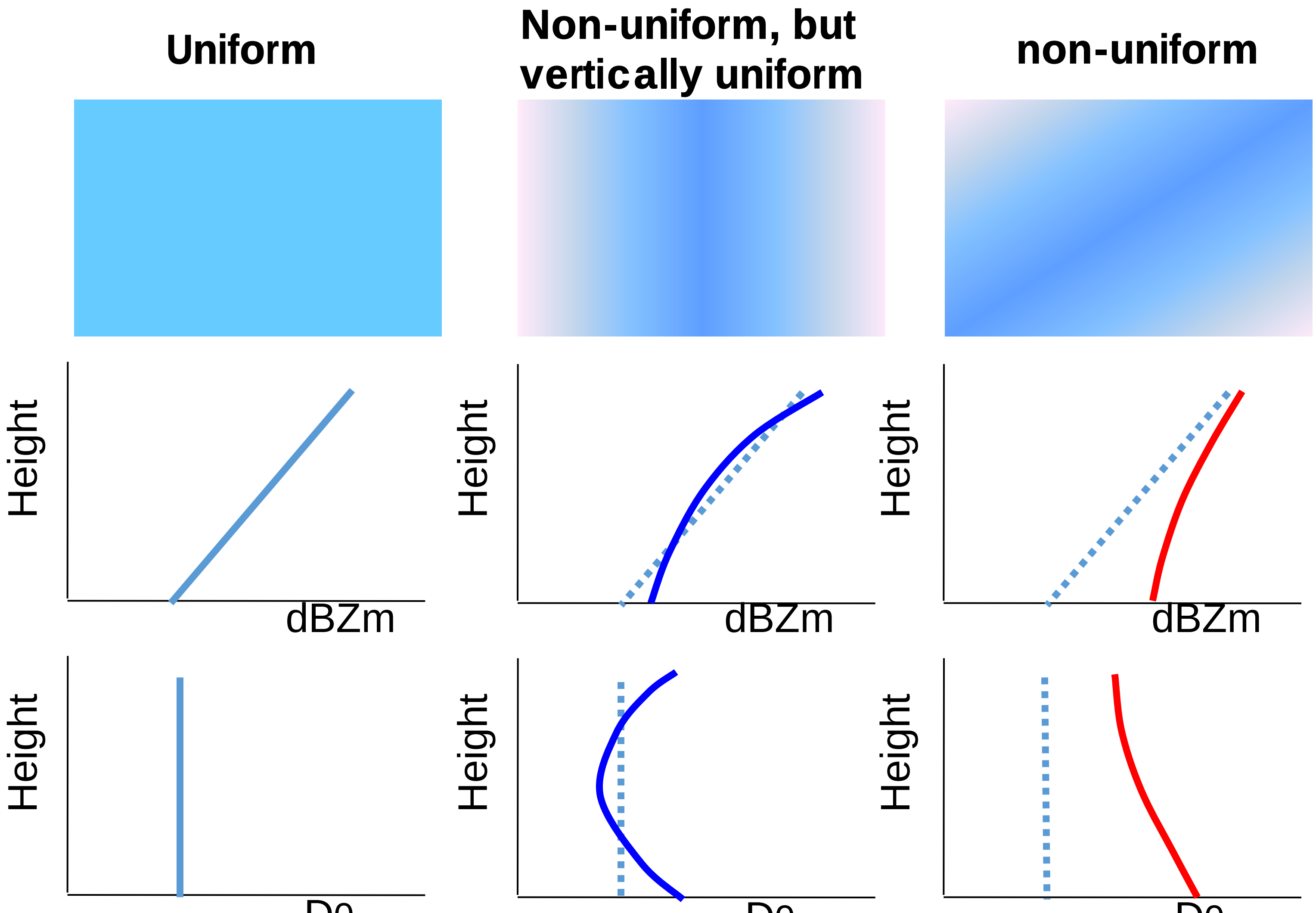

Passive Microwave Retrievals

Column integrated water vs rainfall rate

Tb's in the low frequency channels of a microwave radiometer are proportional to the column integrated rain water content.

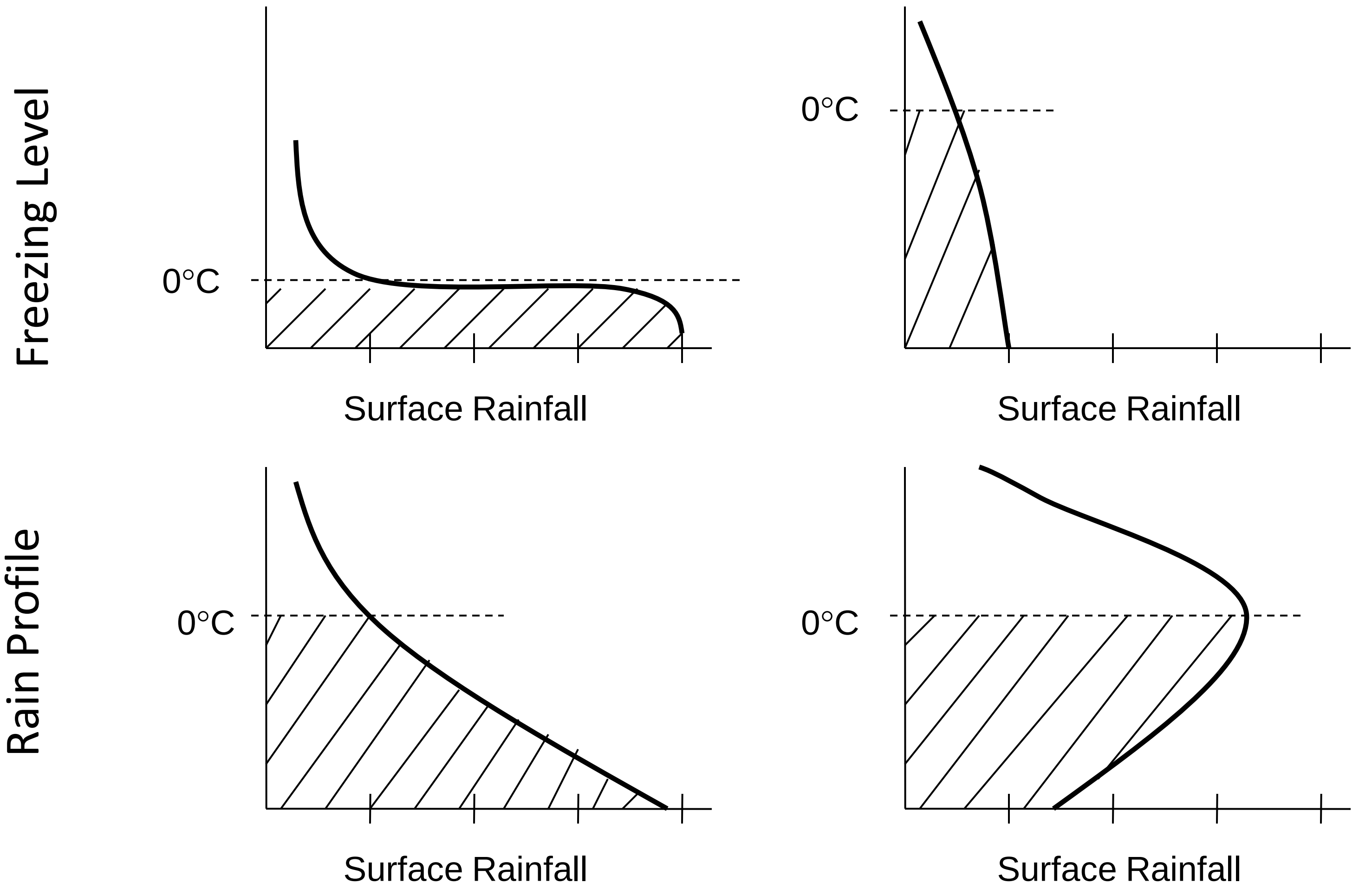

(W. Berg)

Difference of mean vertical rain profile between eastern and western Pacific

Stratiform/Convective Rain Profiles

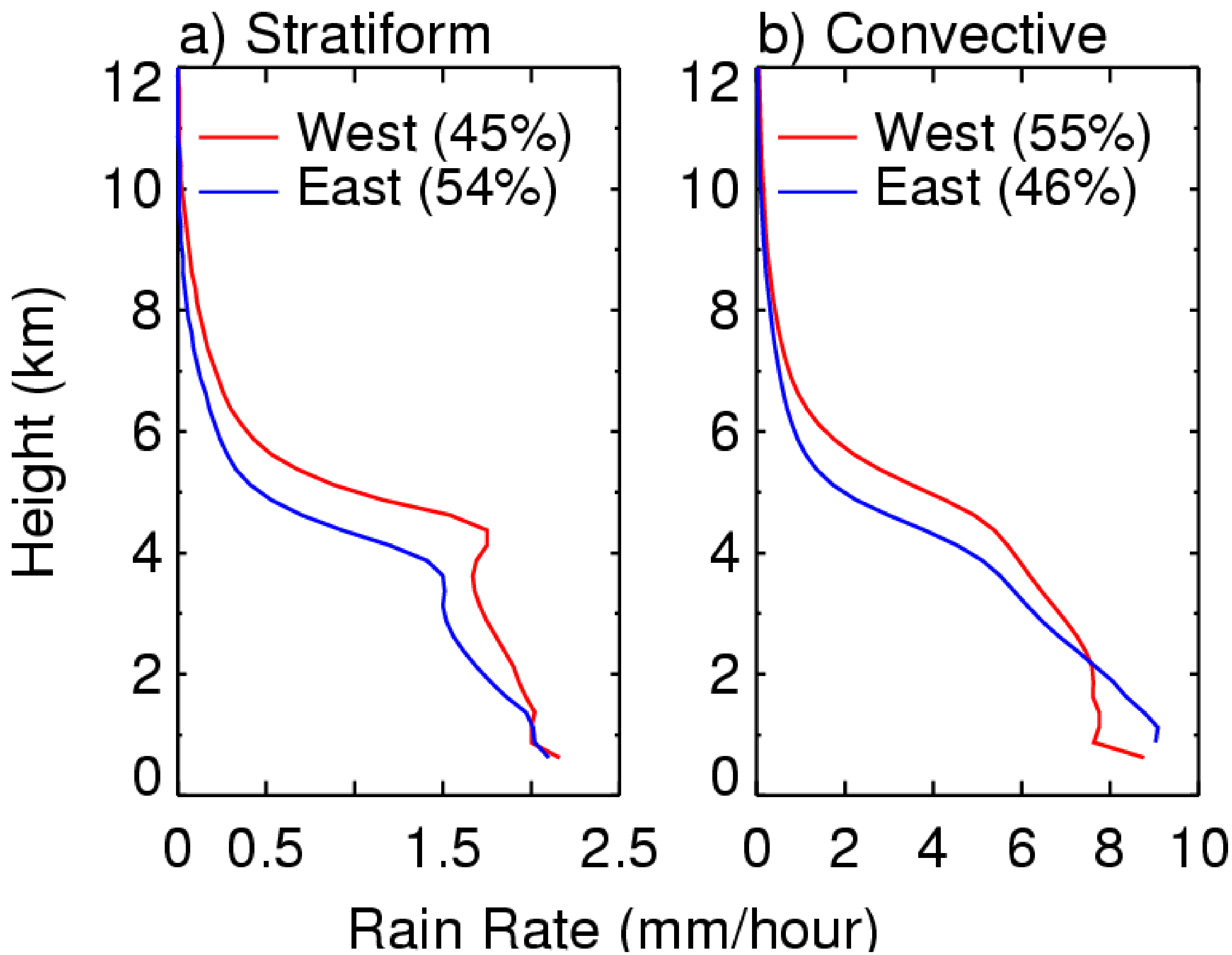

(W. Berg)

PR and TMI Regional Validation

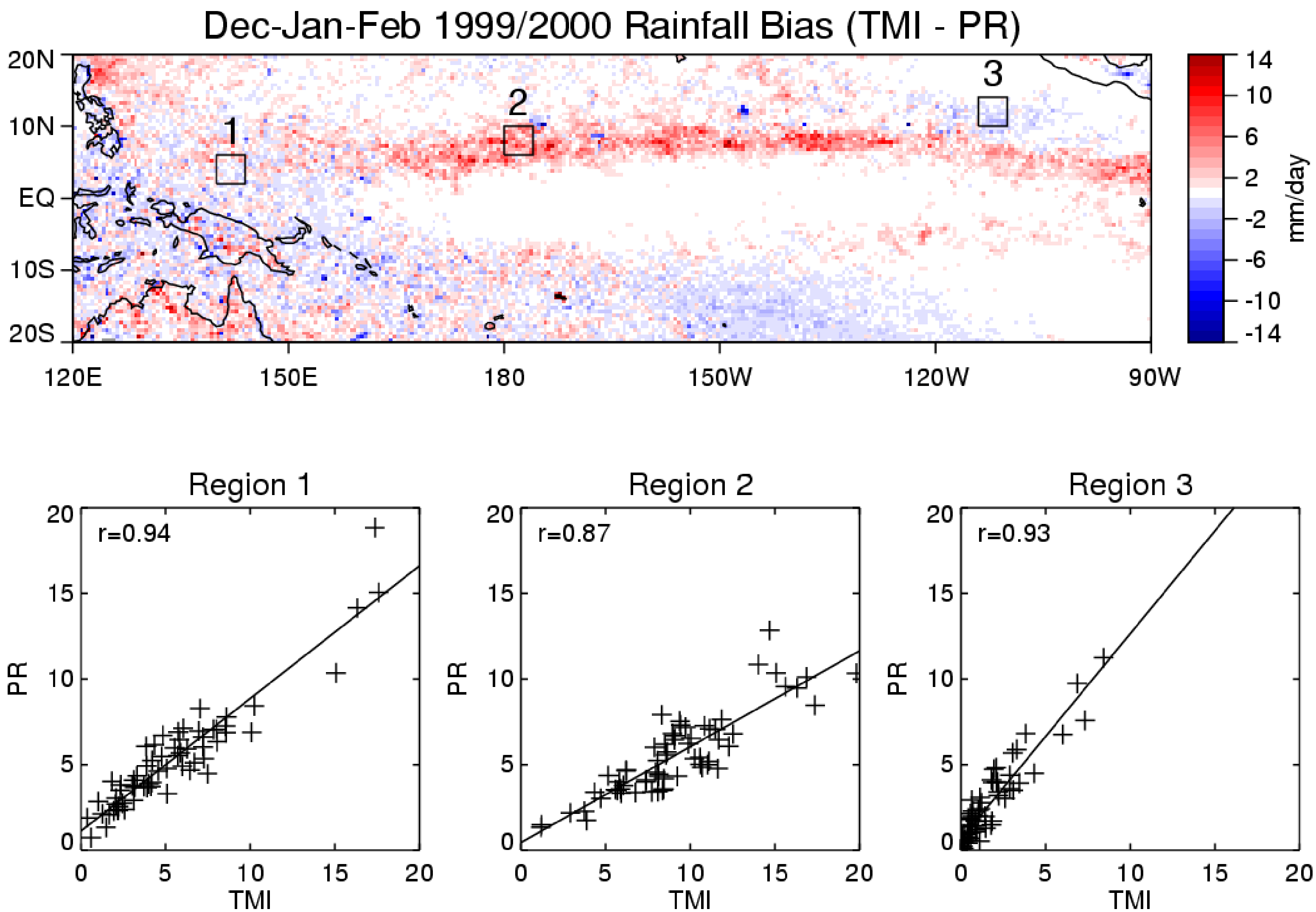

TMI V6, PR V5

(W. Berg, et al.)

Agreement with TMI

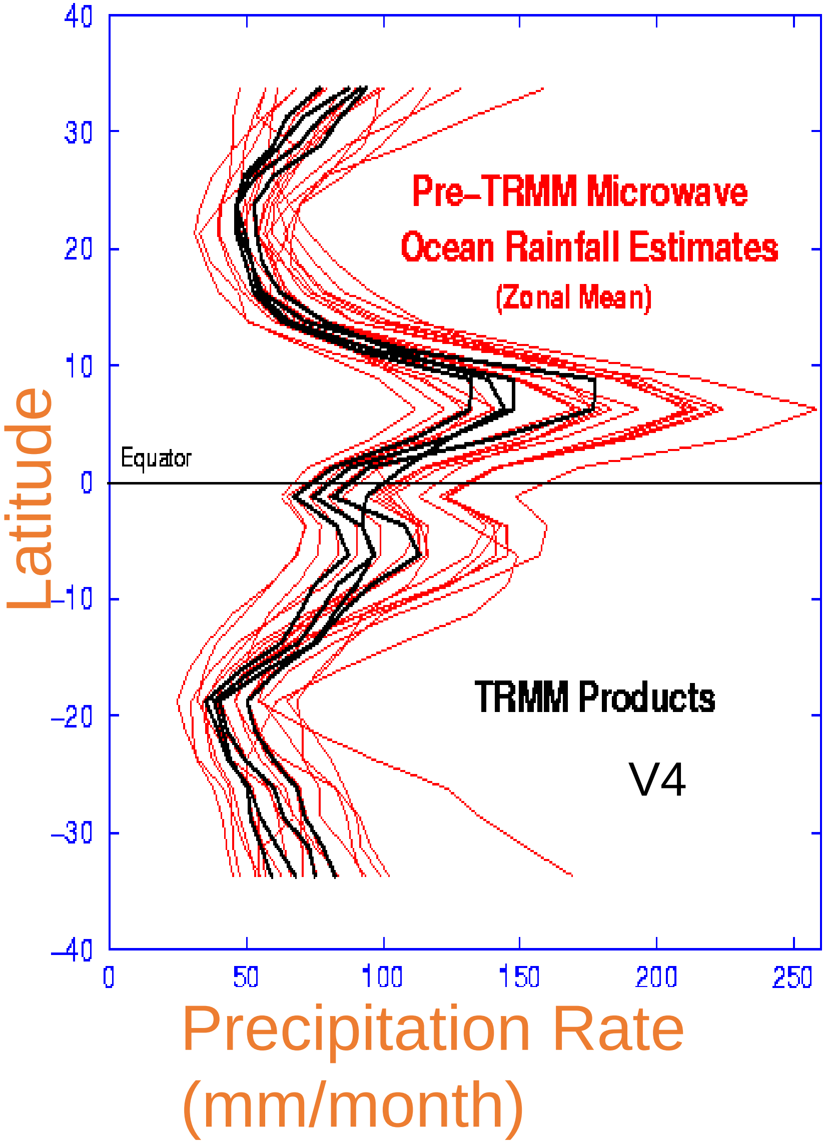

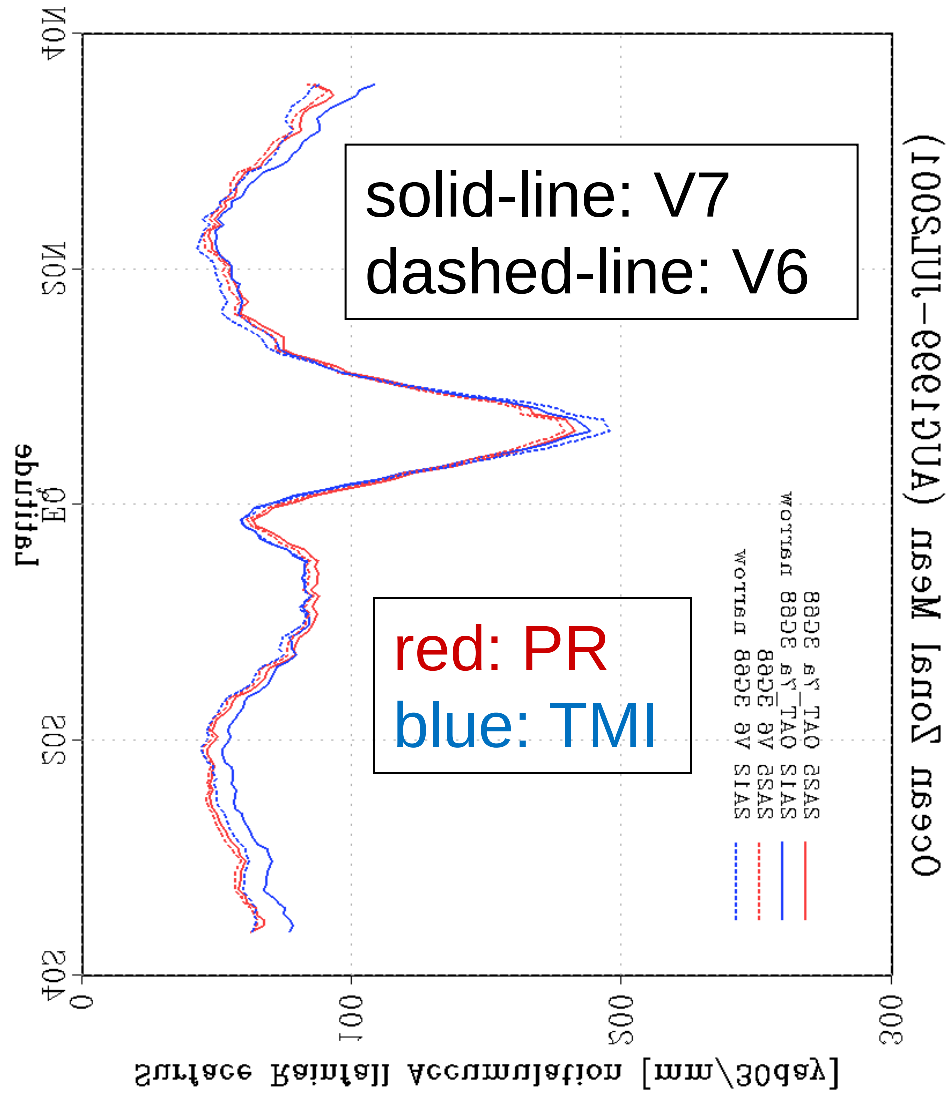

TRMM’s Achievements

- Demonstration of the world’s first space-borne precipitation radar technology
- Scientific Achievements
  - Accurate observation of rain distribution in tropical and sub-tropical regions
  - Diurnal, annual, and long-term variations of precipitation
  - 3-dimensional rain structure (PR)
  - Accurate rain observations over ocean and land with equal quality (PR)
  - Improvement in weather forecasting with 4-D data assimilation
  - Sea Surface Temperature (SST) estimation through clouds
  - Estimation of soil moisture (PR)
- Successful cooperation between US and Japan

Scientific and Social Significance of GPM

Precision brought by DPR

- High sensitivity to detect weak rain and snow
- Accurate estimation of rainfall rate
- Separation of snow from rain
- Progress in cloud physics

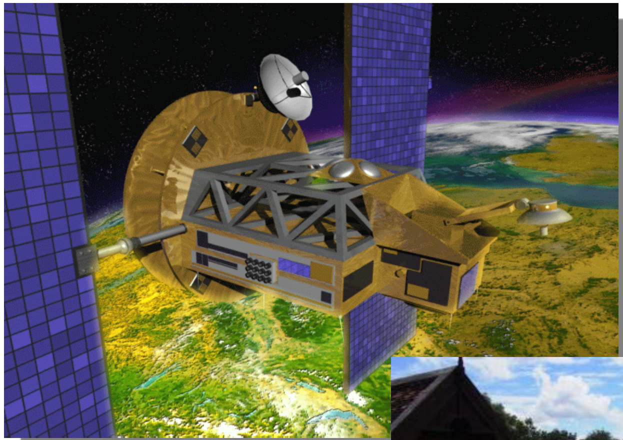

Global rain map in every 3 hours by GPM

- Climate change assessment

  monitor variations in rainfall and rain areas associated with climate changes and global warming
- Improvement in weather forecasts

  Quasi-real-time assimilation of data in numerical prediction models,

  Improved flood prediction
- Water resource management

  river, dam, agricultural water, etc.
- Agricultural production forecasting

GPM(Global Precipitation Measurement)

Purpose

Based on the incredible success of TRMM, GPM was planned to contribute for operational use of precipitation data (High accuracy and Temporally dense global precipitation data set). e.g. 3 hourly global precipitation dataset.

Method

(1) Gain the global coverage and temporally dense observation by multiple passive microwave imagers contributed from space agencies/operational agencies (JAXA, NASA, NOAA, etc.)

(2) Accurate precipitation observation by the Core Satellite equips DPR and microwave imager.

Observation system

Core satellite (Radar + Microwave imager) and Constellation satellites (imager or sounder)

Core Satellite (JAXA-NICT, NASA)

- Dual frequency precipitation radar(DPR)
- GPM Microwave imager (GMI)

✧Accurate precip. observation

✧Calibration to the passive microwave observation (constellation satellites)

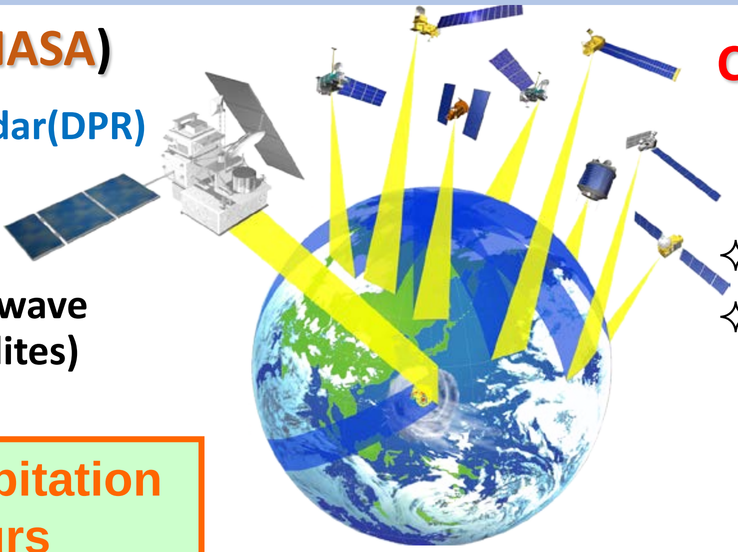

Constellation satellites (NOAA, NASA, JAXA, etc.)

✧Microwave imager or sounder

✧High frequency observation

Produce global precipitation map every 3 hours

Concept of precipitation measurement by the GPM core satellite

Dual-frequency precipitation radar (DPR) consists of
Ku-band (13.6GHz) radar : KuPR
and
Ka-band (35.5GHz) radar : KaPR

JAXA and NICT (Japan) :
DRP (KuPR and KaPR)
Launcher
NASA (US) :
Spacecraft, GMI

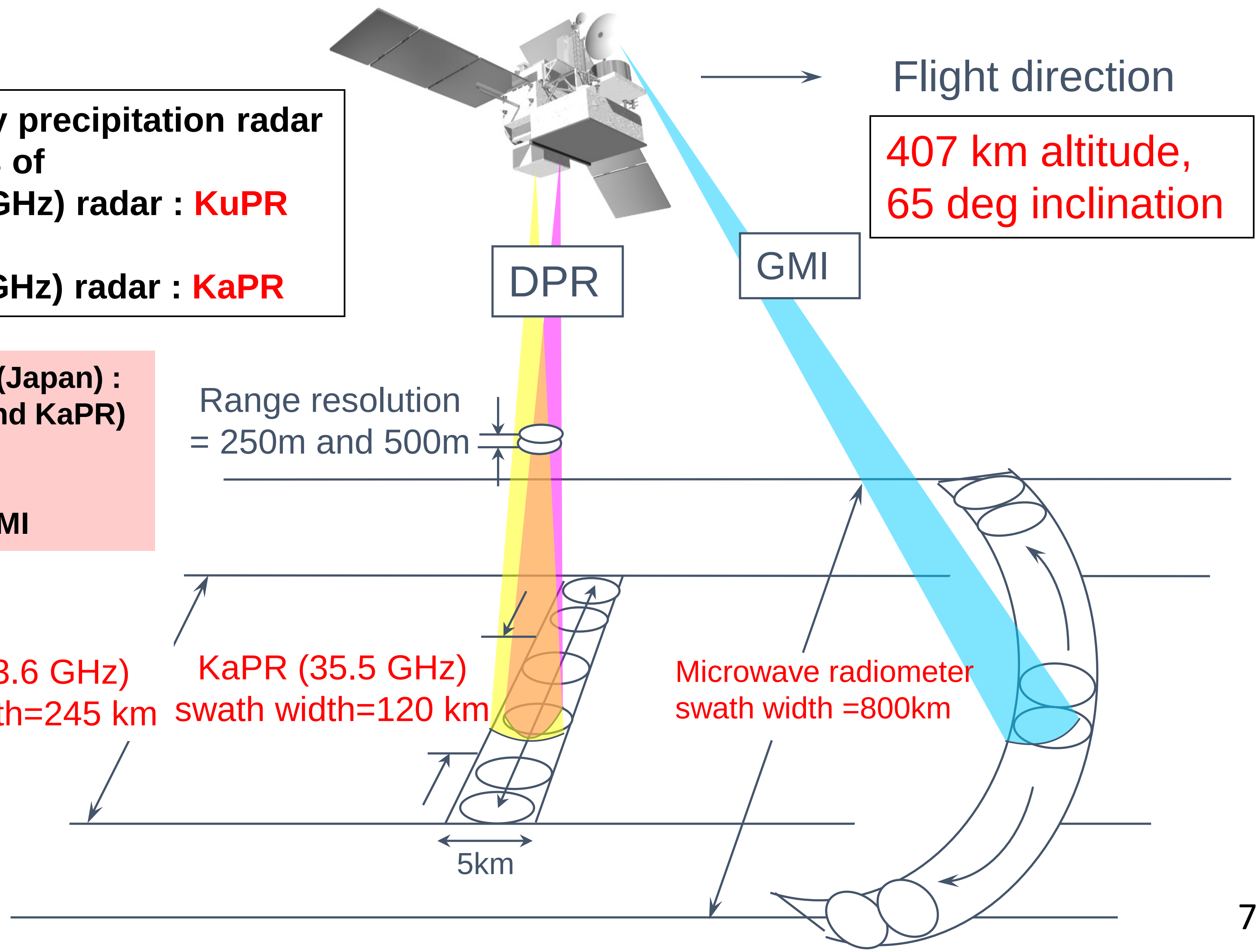

Main Characteristics of DPR

Item	GPM DPR		TRMM PR
	KuPR	KaPR	
Antenna Type	Active Phased Array (128)	Active Phased Array (128)	Active Phased Array (128)
Frequency	13.597 & 13.603 GHz	35.547 & 35.553 GHz	13.796 & 13.802 GHz
Swath Width	245 km	120 km	215 km
Horizontal Reso	5 km (at nadir)	5 km (at nadir)	4.3 km (at nadir)
Tx Pulse Width	1.6 μs (x2)	1.6/3.2 μs (x2)	1.6 μs (x2)
Range Reso	250 m (1.67 μs)	250 m/500 m (1.67/3.34 μs)	250m
Observation Range	18 km to -5 km (mirror image around nadir)	18 km to -3 km (mirror image around nadir)	15km to -5km (mirror image at nadir)
PRF	VPRF (4206 Hz±170 Hz)	VPRF (4275 Hz±100 Hz)	Fixed PRF (2776Hz)
Sampling Num	104～112	108～112	64
Tx Peak Power	> 1013 W	> 146 W	> 500 W
Min Detect Ze (Rainfall Rate)	< 18 dBZ (< 0.5 mm/hr)	< 12 dBZ (500m res) (< 0.2 mm/hr)	< 18 dBZ (< 0.7 mm/hr)
Measure Accuracy	within ±1 dB	within ±1 dB	within ±1 dB
Data Rate	< 112 Kbps	< 78 Kbps	< 93.5 Kbps
Mass	< 365 kg	< 300 kg	< 465 kg
Power Consumption	< 383 W	< 297 W	< 250 W
Size	2.4×2.4×0.6 m	1.44 ×1.07×0.7 m	2.2×2.2×0.6 m

* Minimum detectable rainfall rate is defined by $Ze=200\,R^{1.6}$ (TRMM/PR: $Ze=372.4\,R^{1.54}$)

Dual Frequency Precipitation Radar

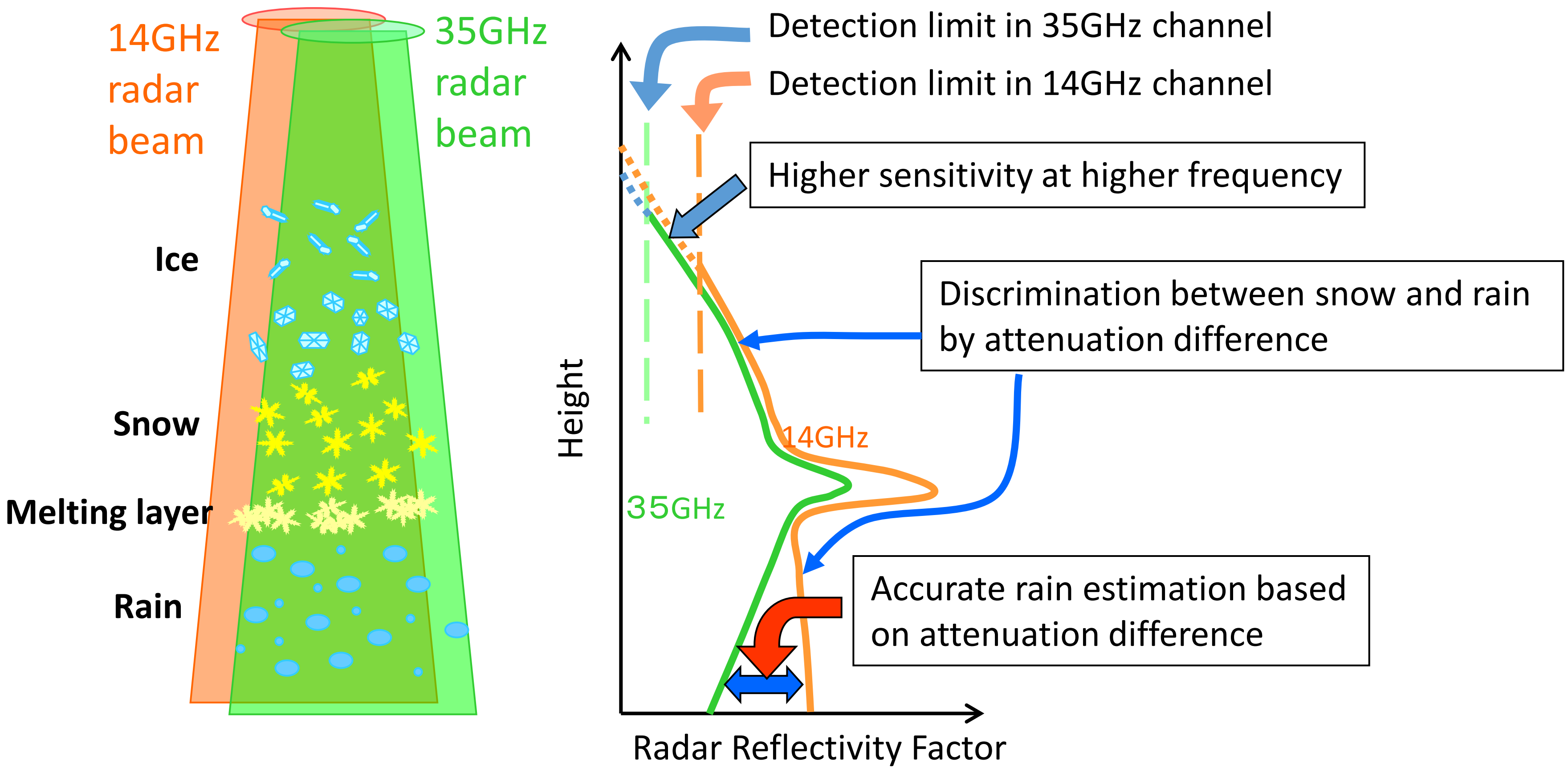

- Measure 3-D structure of rain as TRMM, but with better sensitivity
- Accumulate climatological precipitation data continuously since TRMM
- **Improve estimation accuracy with dual-frequency radar**
  - Identification of hydrometer type
  - Estimation of DSD parameters

GPM DPR algorithm development

- Basic flow is the same with TRMM PR
  - Judge the storm type (convective or stratiform)
  - Estimate phase state of precipitation at each height
  - Attenuation corrections to estimate Z_e(Ka) and Z_e(Ku)
  - Combine Z_e(Ka) and Z_e(Ku) to estimate 2 DSD parameters
- New information from GPM DPR
  - Z_m profiles at two frequencies
  - σ^0 (or PIA estimate) at two frequencies (σ^0(Ka) and σ^0(Ku))
  - Denser horizontal samples in Ka band (interlaced scans)
  - higher sensitivity
  - larger observation area (high latitudes)

Special Concerns in Rain Profiling Algorithms for DPR

- Attenuation correction is essential
  - Attenuation by precipitation is not negligible.
    - In particular, Ka-band radar
    - *k-Z* relation for rain attenuation (H-B solution)
  - Attenuation by CLW and WV is not negligible.
    - **Cloud liquid water: Att(Ka) = 10 * Att(Ku), up to 5 dB**
    - **Water vapor: Att(Ka) = 5 * Att(Ku), up to 1.5 dB near surface**
    - **Oxygen: Att(ka) = 5 * Att(Ku), 0.4 dB near surface**
  - Use of surface reference technique (SRT) helps.
    - But, SR is not always available or reliable
- Type of particles (rain, snow, graupel, etc.) and their physical and electromagnetic properties need to be known (or assumed).
- Inhomogeneity of rain within IFOV
  - Entangled with apparent attenuation, etc.

GPM/DPR level-2 algorithm flow (V05)

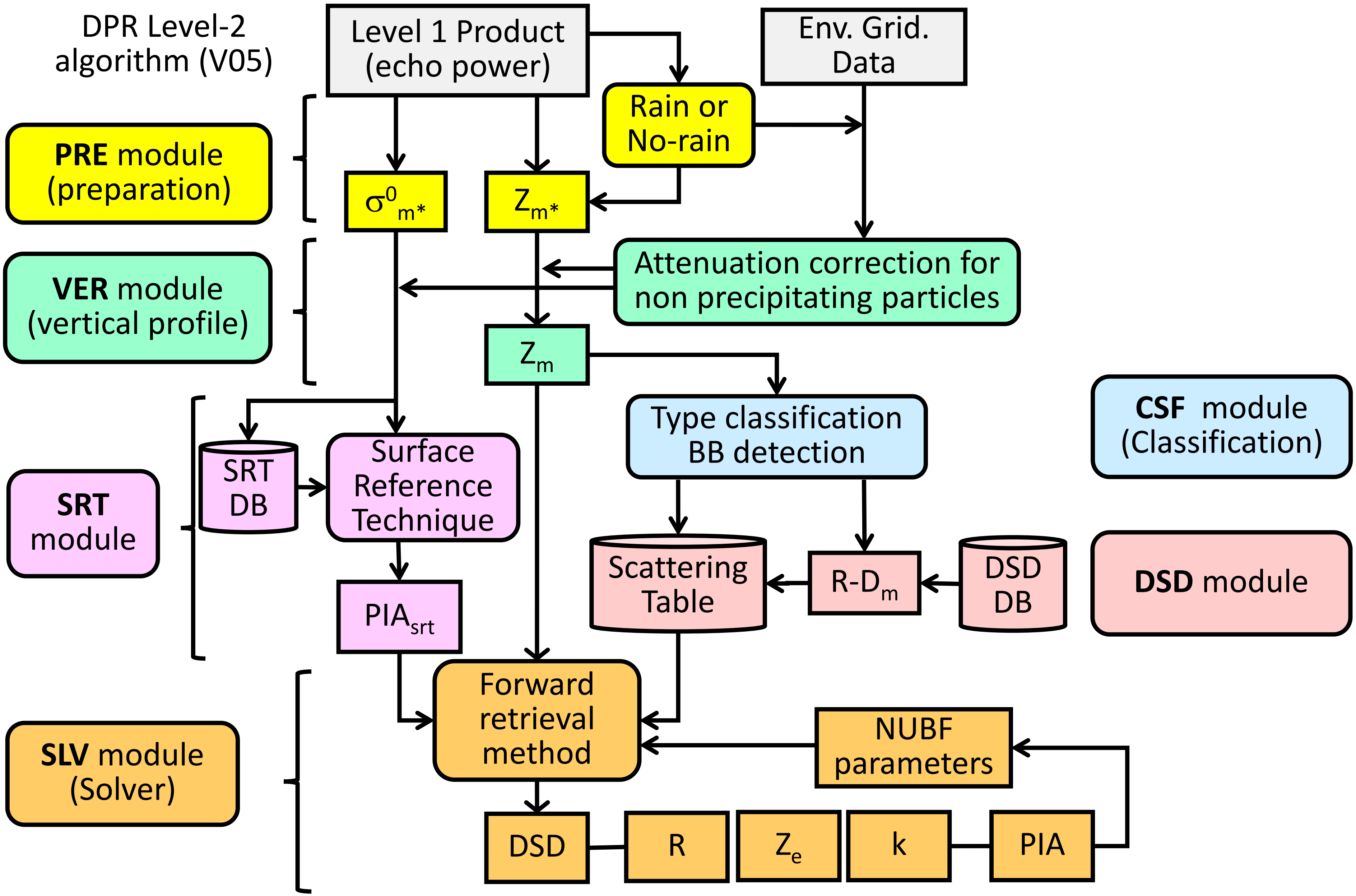

Basic Idea of Meneghini's DF Algorithm

- $2N(+2)$ observables ($2N$ of Zm (and 2 of $\Delta\sigma^0$)) to estimate RR at N range gates.
  - If the relations among Z, R and k were constant, R would be overdetermined.
  - In fact, Z, R and k are functions of many parameters (DSD, phase, shape, temp., vertical air velocity, non-uniformity, etc.)
- Parameterize DSD with two variables.
  - E.g., N_0 and D_0、 N_0^* and D_0
- Estimate these two parameters at each gate.
  - $2N$ estimates from $2N(+2)$ observables
- All other parameters are fixed.
  - E.g. shape parameter in DSD, phase, temp, etc.
- Calculate R with the estimated parameters.
- Needs initial conditions (e.g., attenuations at a range)

$$N(D) = N_0 f(D : D_0)$$

$$Z_{e\lambda} = c_{Z\lambda} \int \sigma_{b\lambda}(D) N(D)\, dD = N_0 I_{b\lambda}(D_0)$$

$$k_\lambda = c_k \int \sigma_{t\lambda}(D) N(D)\, dD = c_k N_0 I_{t\lambda}(D_0)$$

$$Z_{m\lambda}(r) = A_\lambda(r) Z_{e\lambda}(r)$$

$$A_\lambda(r) = \exp\left(-\frac{2}{c_k}\int_0^r k_\lambda(s)\, ds\right)$$

At each range, r,

$$Z_e(r;Ka)/Z_e(r;Ku) \Rightarrow D_0(r)$$

$$Z_e(r;Ku),\ D_0(r) \Rightarrow N_0(r)$$

$$D_0(r),\ N_0(r) \Rightarrow R(r),\ k(r;Ka),\ k(r;Ku)$$

Range r to $r+\Delta r$

$$k(r;Ka),\ Z_e(r;Ka),\ Z_m(r+\Delta r;Ka) \Rightarrow Z_e(r+\Delta r;Ka)$$

$$k(r;Ku),\ Z_e(r;Ku),\ Z_m(r+\Delta r;Ku) \Rightarrow Z_e(r+\Delta r;Ku)$$

Iterate

Dual-Frequency Ratio (DFR) for snow

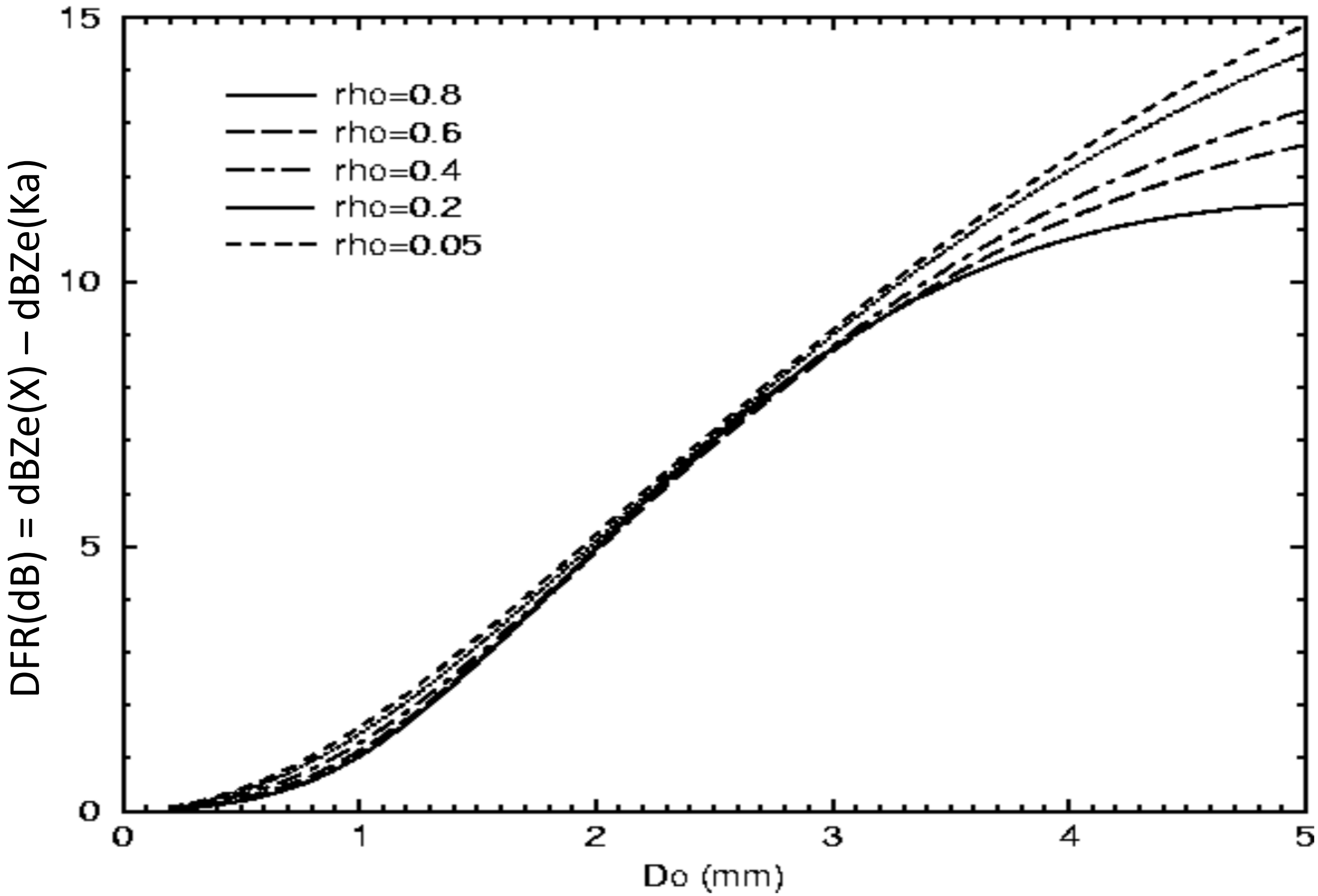

DFR at X and Ka bands versus snow D_0 for several snow densities for μ equal to 2.

(Liao et al. 2003)

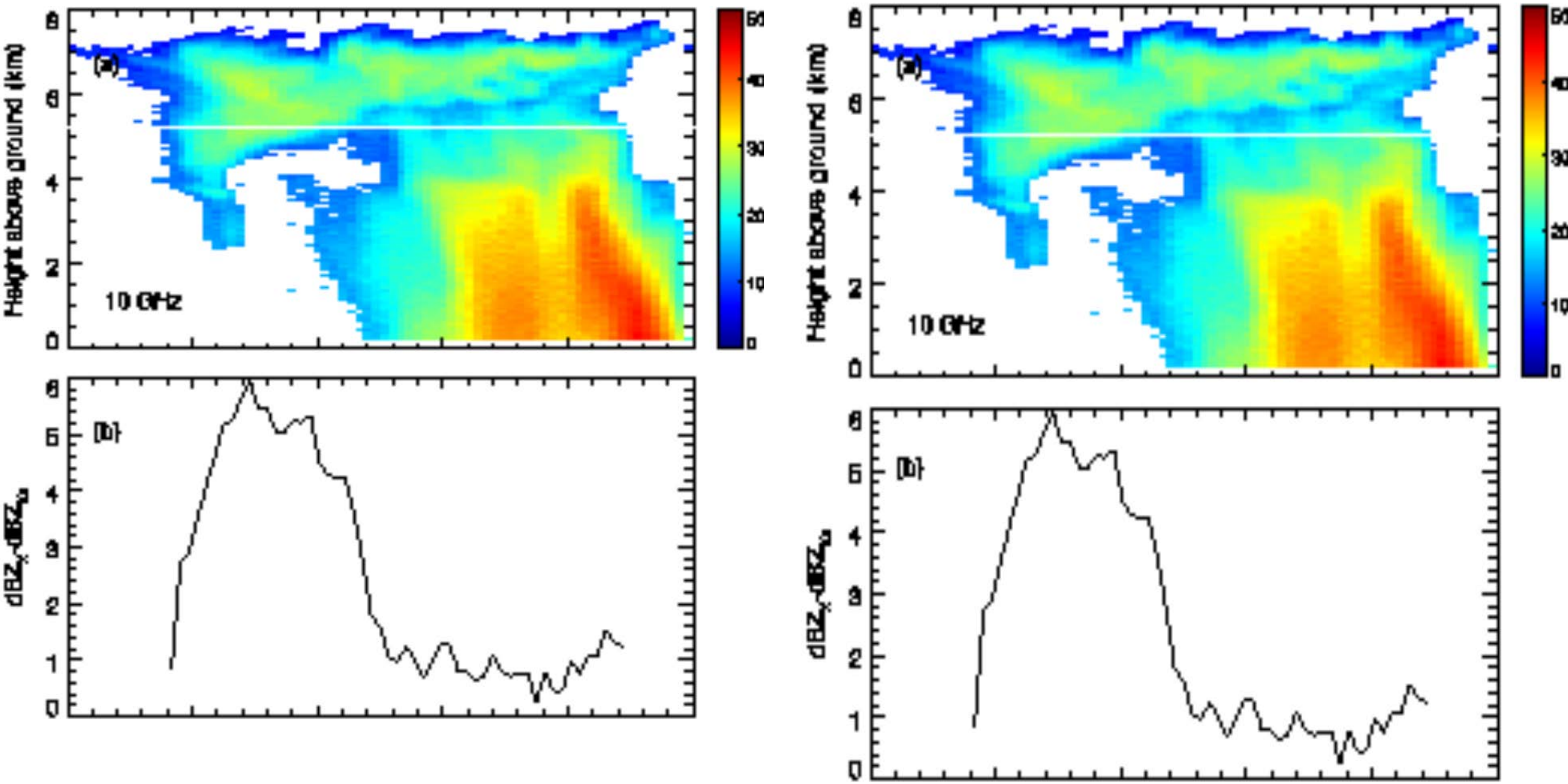

Airborne radar measurements over a weak convective cell and retrievals of the size distributions in comparisons with the in-situ particle measurements: (a) T-39 radar measured reflectivity at nadir along the flight track shown in Fig.2, (b) DFR of X and Ka bands at the altitude where the T-28 flew, as indicated by the white line in Fig.3a, (c) comparisons of D_0 between the radar estimated and the 2D-P measured results and (d) similar comparisons for N_T.

(Liao et al. 2003)

Characteristics of DF algorithm (Ze-ratio method)

- can estimate **two DSD parameters** at each range bin.
- generally works well under the given assumptions (SRT available, no NUBF effect, etc.)
  - Random noise or quantization error in P_r does not cause a serious bias error in retrieval.
- Issues:
  - Multiple solutions possible for liquid particles
  - **Choice of DSD model** (Closeness of model DSD to actual DSD)
    - Actual variation of DSD is rather large (A. Tokay, N. Adhikari)
  - separation of solid (ice) phase from liquid phase
  - inhomogeneity of rain within footprint
  - beam mismatching
  - attenuation caused by CLW and water vapor

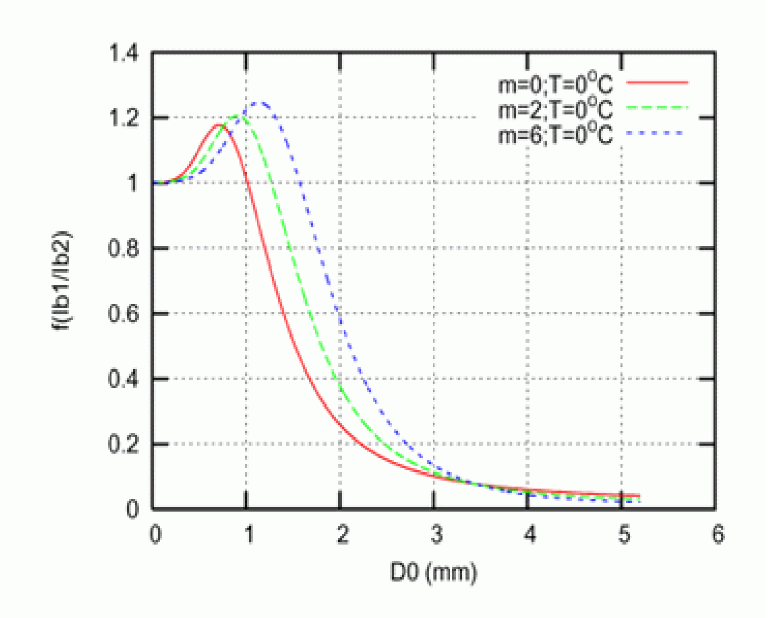

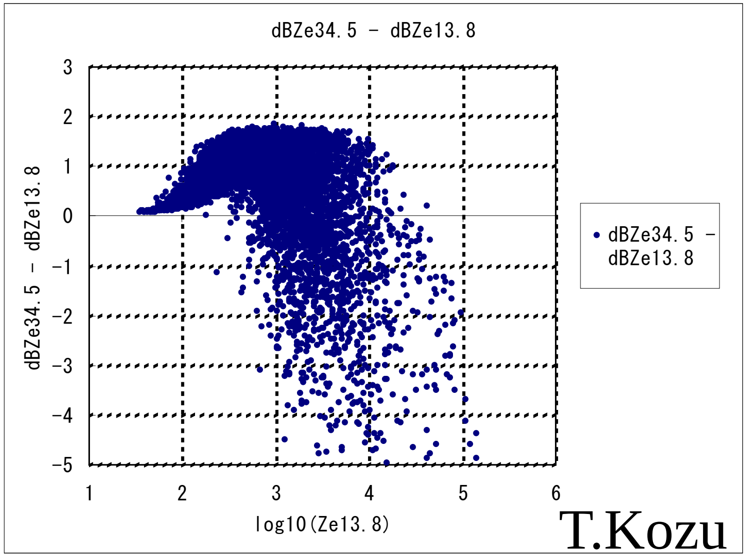

T.Kozu

Convective, 1<R(mm/h)<3.2

(S. Seto)

PR

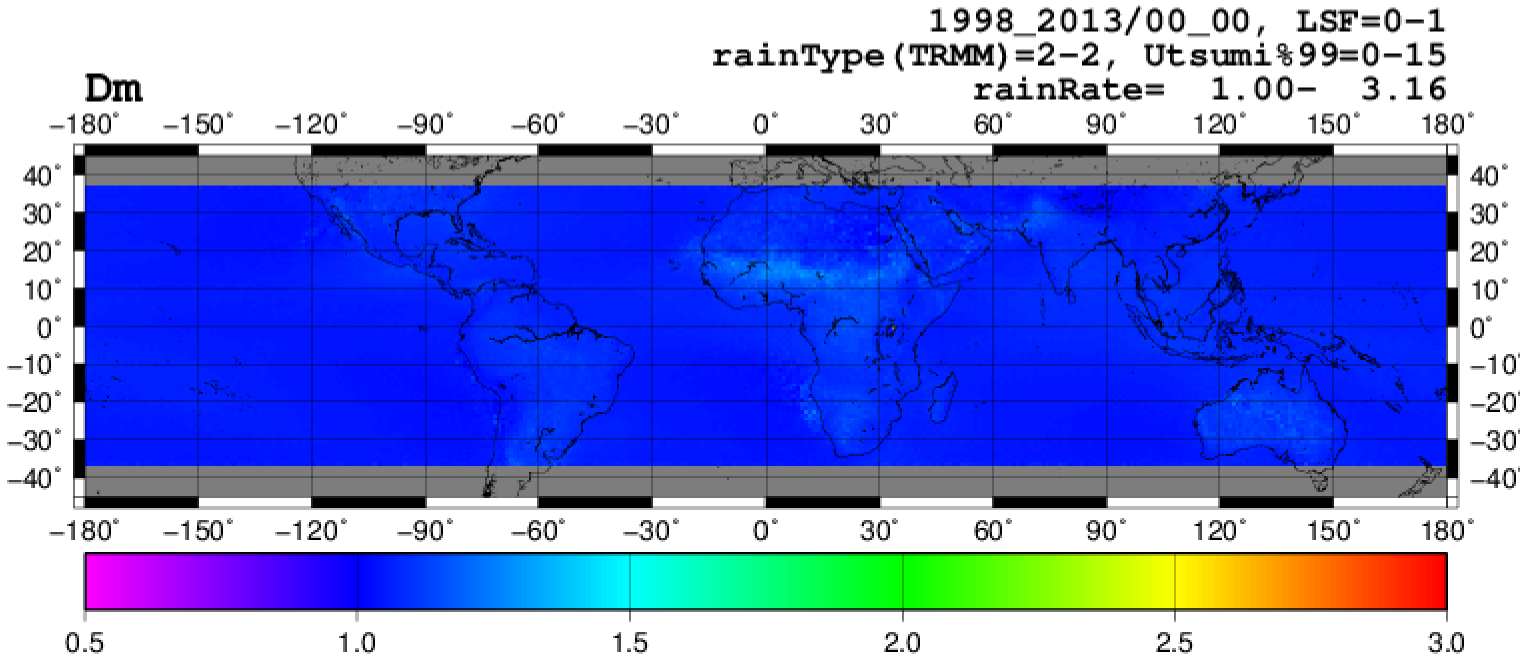

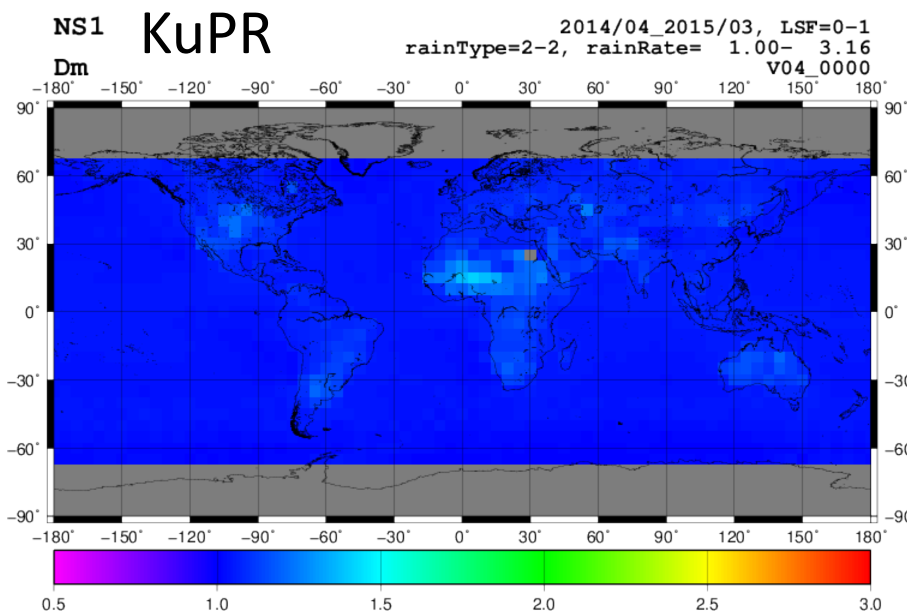

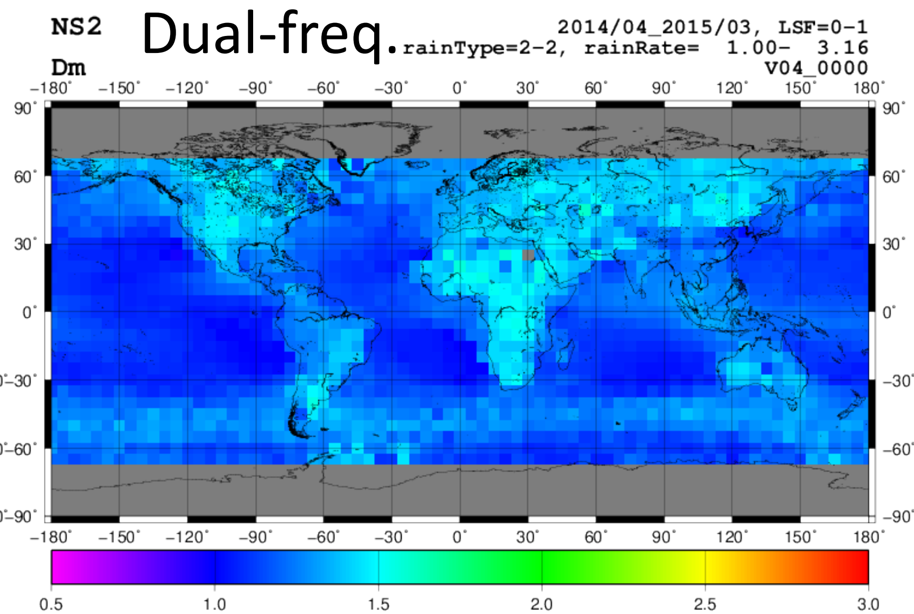

Gadanki, India

(S. Seto)

0.32<R<1 1<R<3.2 3.2<R<10 10<R<32 32<R<100

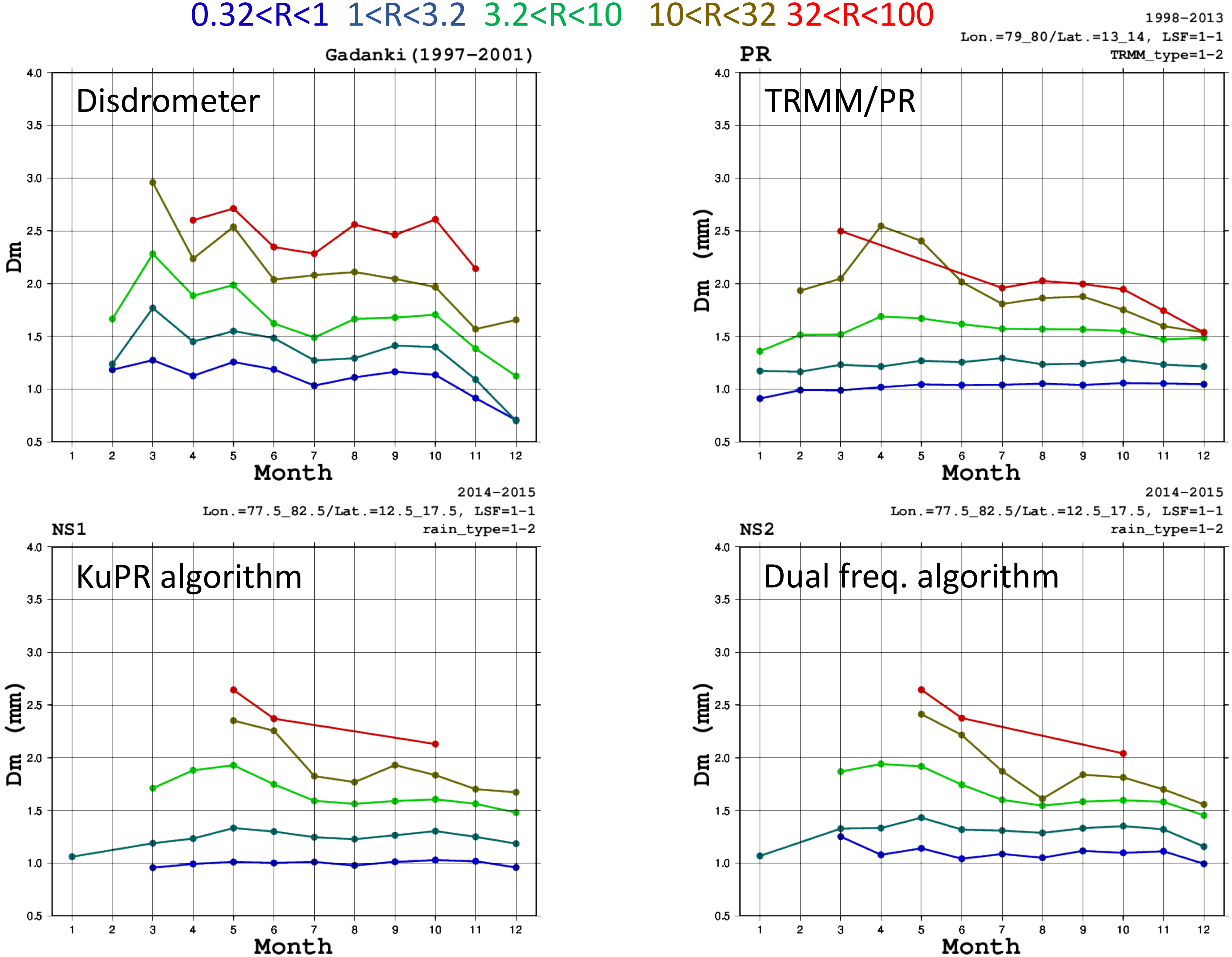

GPM V5 Test Products

(J. Kwiatkowski)

KuMS is the Ku ifovs within the DPR MS scan

Ocean

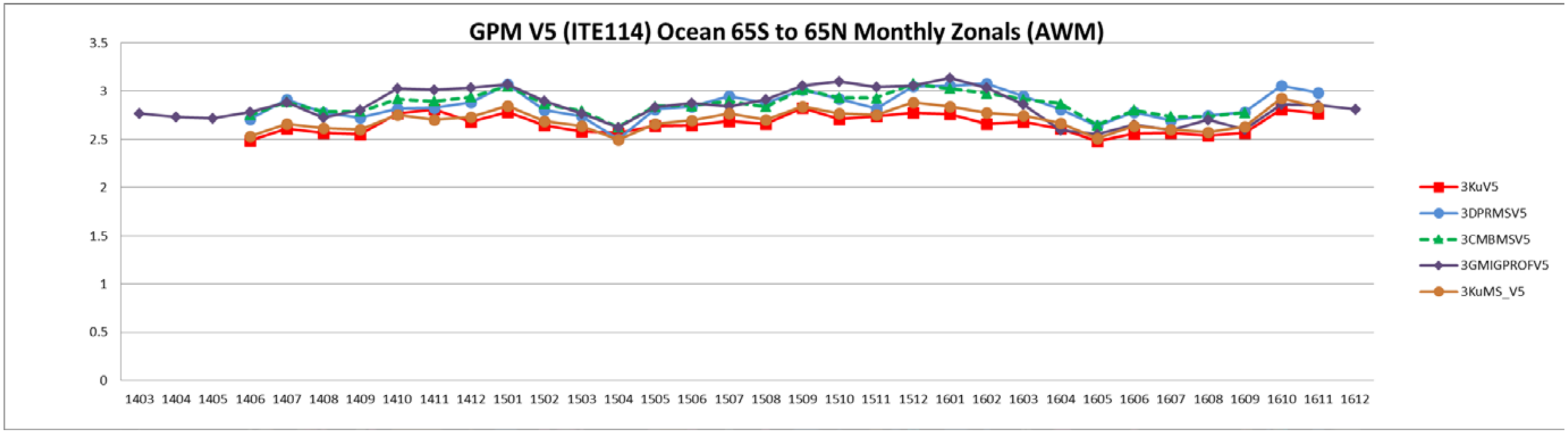

Land

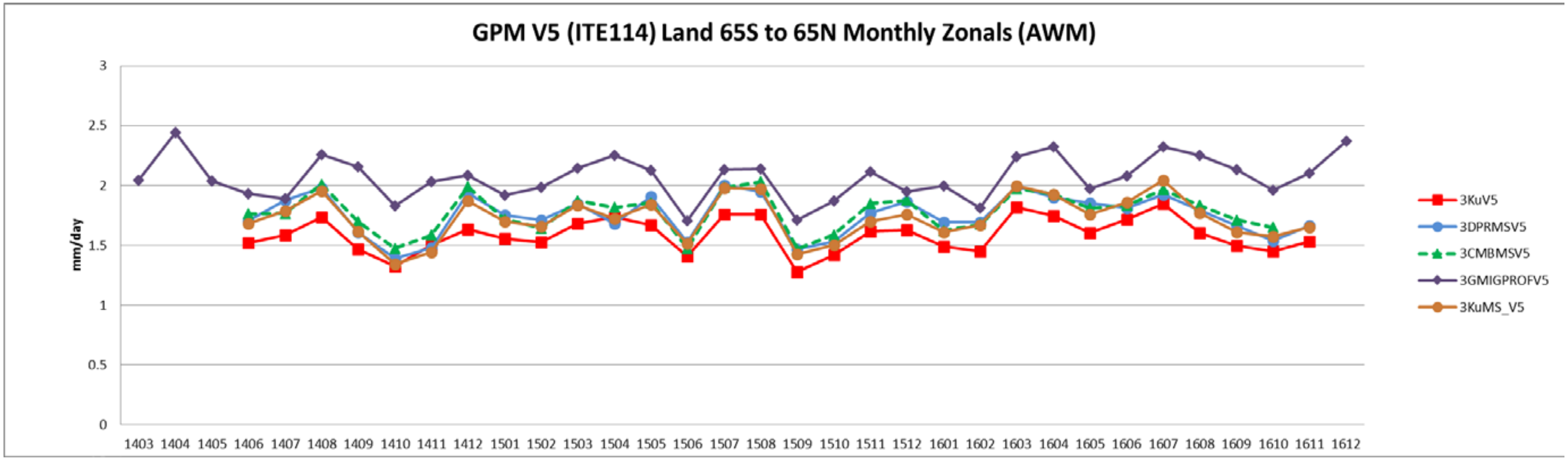

2-Year Zonals V5

(J. Kwiatkowski)

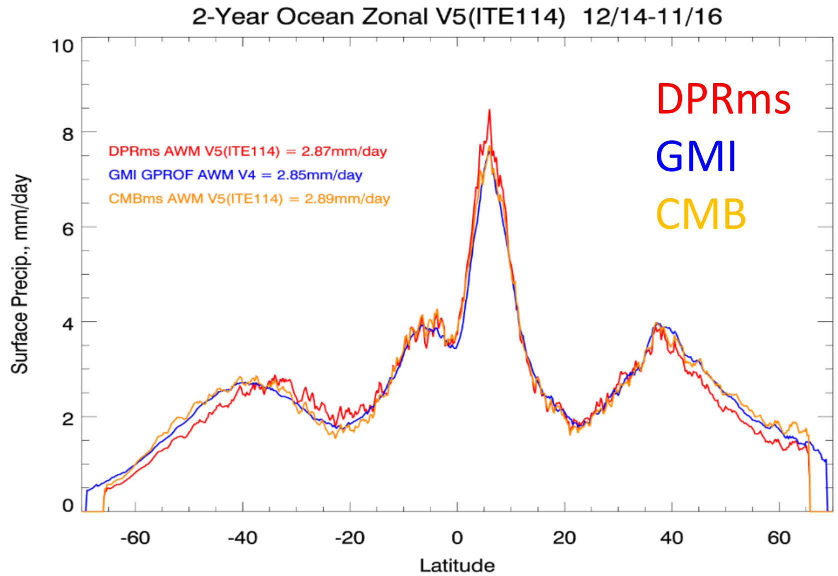

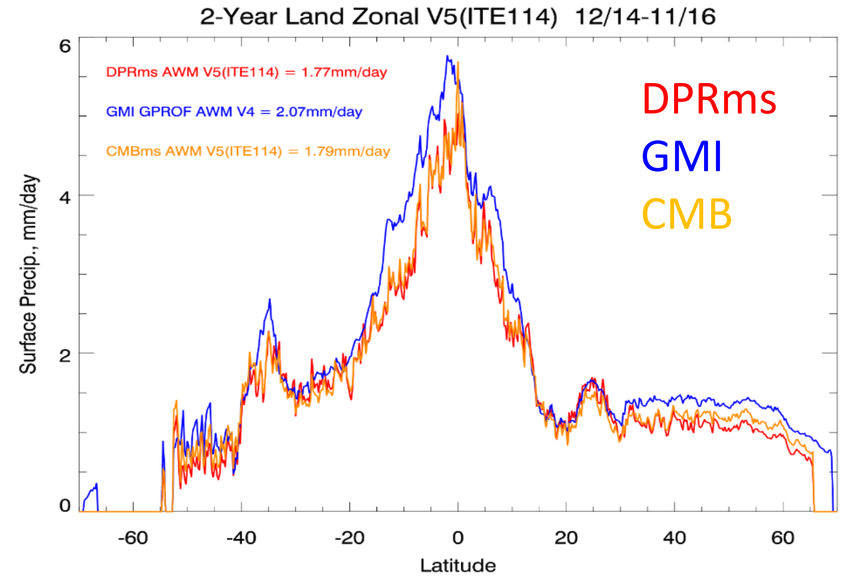

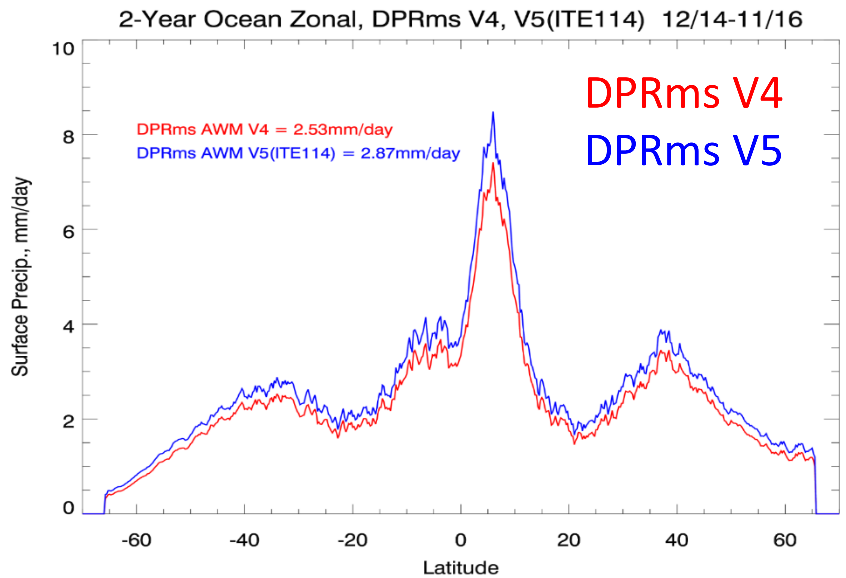

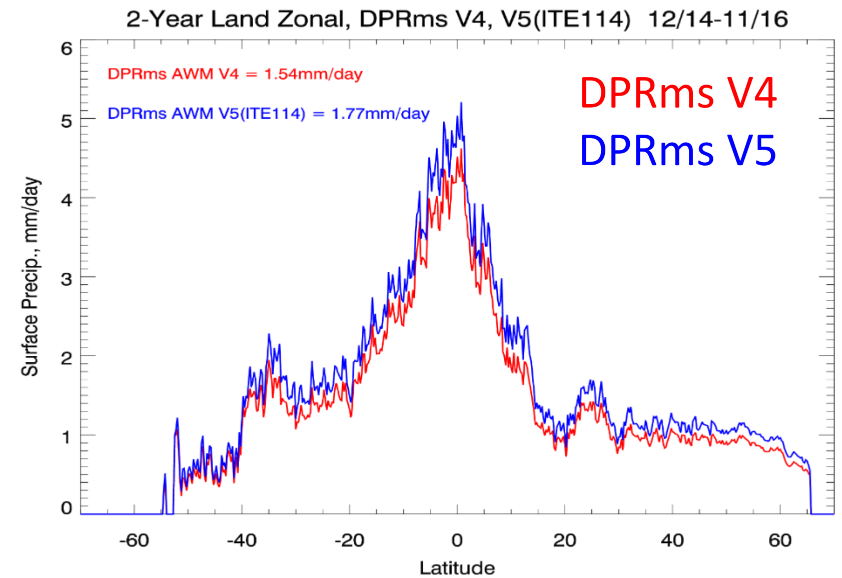

Comparisons of KuPR rain estimates with AMeDAS rain gauge data

(KuPR – Gauge)/Gauge

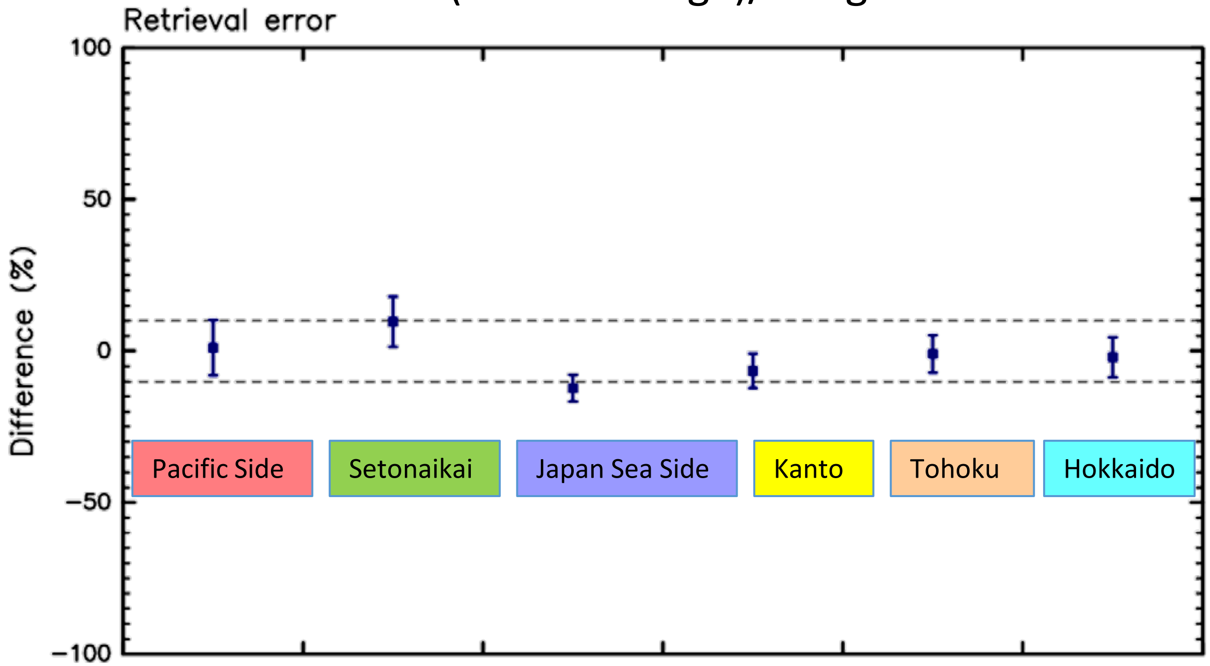

6 areas

1. Hokkaido (No. of boxes: 45)
2. Tohoku (34)
3. Kanto (27)
4. Sea of Japan side (27)
5. Inland Sea area (27)
6. Pacific Ocean side (39)

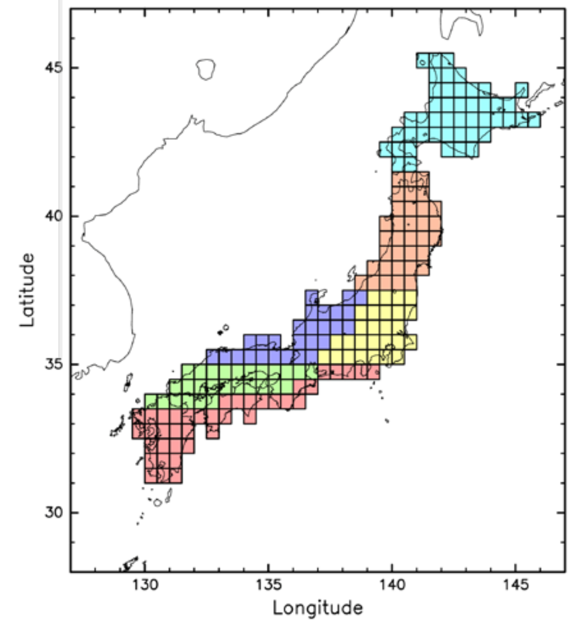

- Two years of data from June 2014 to May 2016
- AMeDAS data at overpasses only
- Gauge data are 10 min data immediately after the overpasses
- Rain total is estimated at each 0.5 × 0.5 deg. box, and means and standard deviations of 6 colored areas are calculated.
- To exclude snow fall data, if the surface temperature is below 6 degrees, data in that box are not used.

(N. Kawamoto)

Zonal rain comparison: DPR(MS) (ITE113) and MRMS MNQ

- June 2014 – May 2015
- MRMS: 0.01 deg, hourly data,
    - DPR overpass time only

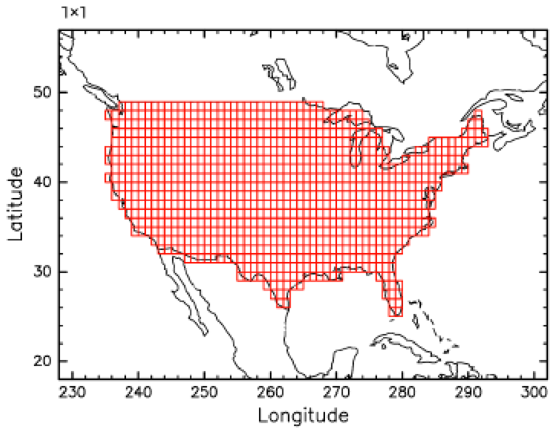

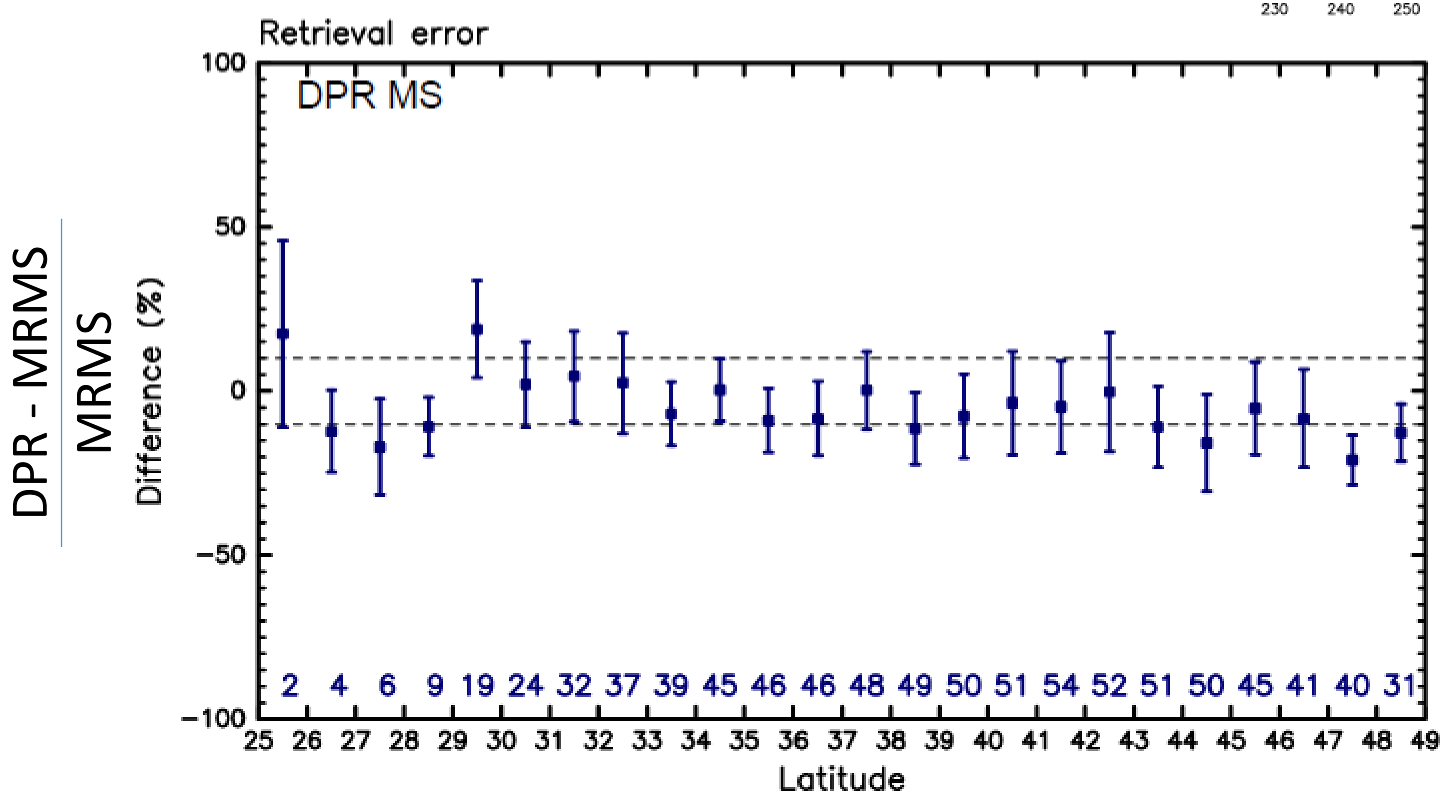

(N. Kawamoto)

Factors that may affect the rain estimates from space-borne radar data

- Principles of radar measurement of rain
  - Conversion of received power (Pr) to apparent radar reflectivity factor (Zm) (Calibration of instrument)
  - Conversion of Zm into effective radar reflectivity factor (Ze) (attenuation correction)
  - Conversion from Ze to rain rate (R)
- Scattering and extinction characteristics of precipitation particles and their vertical distribution (Type of precipitation: rain, snow, groupel, hail, etc.)
  - Drop size distribution (DSD)
  - Phase state, density (Mixing formula)
  - Shape and canting angle
  - Temperature (refractive index)
- Fall velocity of precipitation particles (size, density, shape, vertical wind)
- Inhomogeneity of rain (Non-uniform distribution of rain)
- Scattering characteristics of sea and land surfaces
- Attenuation due to constituents other than precipitation itself
  - Clouds, water vapor, other gasses
- Effect of multiple scattering (Ka band and above)

Future Issues

- Statistics of PSD (Particle Size Distribution) shows a clear difference between rain over ocean and rain over land.
  - The current algorithm assumes common PSD parameters over ocean and land for each storm type.
  - There are more small drops than the assumed PSD over ocean and the opposite over land.
  - Possibility of defining regionally dependent PSD models from the knowledge we accumulated in the past.
- Orographic rain.
  - Vertical structure of orographic rain may differ substantially from other types of rain.
  - Estimating surface rain from the rain echoes at altitude much higher than the surface involves a large error.
  - Poor performance of SRT in mountainous regions amplifies the issue.
- Non-uniformity of rain distribution within a footprint remains to be a very complex but important issue to be solved in the future.

Summary

- TRMM/PR realized radar measurement of precipitation from space for the first time.
- Both TRMM/PR and GPM/DPR provide us with 3D distribution of precipitation globally (but with limited space-time sampling).
- Comparisons of radiometer data with radar data improved the rain retrieval algorithm of radiometer substantially.
- TRMM and GPM data are used in many fields of scientific study and practical applications.
- Improvement of precipitation retrieval algorithms need improved knowledge of microphysics and storm structures.
- Collaborations between algorithm developers and data assimilators will benefit the progress in improvement of studies in both fields.


Thank you for your attention